AN ELECTRICAL RESISTIVITY SURVEY OF THE PUNA AND KAU DISTRICTS, HAWAII COUNTY, HAWAII

July 31, 1973

Carried out for:

The Research Corporation of the
University of Hawaii,
Honolulu, Hawaii

GROUP SEVEN

EXHIBIT 140

AN ELECTRICAL RESISTIVITY SURVEY OF THE PUNA AND KAU DISTRICTS, HAWAII COUNTY, HAWAII

Abstract

An electrical resistivity survey was carried out over the Kilauea shield area in Puna and the Kau district of the Island of Hawaii during the period from May through July, 1973, for the purpose of locating areas favorable for the presence of geothermal reservoirs. The technique employed was the dipole mapping technique, which is widely used as a reconnaisance method in prospecting for geothermal reservoirs. It was found that the flanks of Mauna Loa are underlain by rocks of high resistivity, and that such rocks probably extend into the Puna area along the projection of an ancient rift zone of the volcano, Mauna Loa. The high resistivities probably represent the presence of dense, cool dike complexes, so that this portion of the area is unlikely to have much prospect for geothermal development. On the other hand, resistivities as low as two ohm-meters were mapped along the lower part of the East Rift of Kilauea. Assuming reasonable values of porosity and water salinity, such resistivity values are compatible with the presence of thermal waters with temperatures above 180° C., probably extending to a depth of two kilometers below sea level. Measurements made around the summit area of Kilauea confirm the existence of a brackish-water geothermal system along the south side of Kilauea Caldera, in the vicinity of the Kilauea Geothermal Test Well. It is recommended that further detailed work be carried out in the vicinity of the areas with anomalously low resistivity in Puna, so that the best location for a test hole may be found.

GROUP SEVEN

AN ELECTRICAL RESISTIVITY SURVEY OF THE PUNA AND KAU DISTRICTS, HAWAII COUNTY, HAWAII

Introduction

During the period from May 20, 1973, to July 31, 1973, an electrical resistivity survey was carried out over the Kilauea Shield area of the Island of Hawaii for the purpose of finding locations possibly favorable for the occurence of geothermal fluids. The areas surveyed lay mainly in the districts of Puna and Kau, County of Hawaii. In addition, a limited series of measurements was made in the South Kohala district, generally in the area between Kamuela and Kawaihae. The surveys were carried out by a group consisting of G. V. Keller, J. J. Skokan, C. K. Skokan, and J. Daniels, geophysicists, and J. Schoemaker and B. Miyamoto, field assistants.

The electrical surveys described in this report were intended to fill the role of reconnaisance, rather than to serve in the role of detailed exploration. The technique used was the dipole mapping technique. In this, an electric field is set up in the earth by passing large amounts of low-frequency current into the earth between a pair of electrode contacts. The electric field developed by this current was then mapped in detail by making measurements of the voltage drop between closely-spaced electrode pairs at many measurement locations in the area around the source bipole. Local increases in the electrical conductivity of the rock, such as are usually associated with the occurence of geothermal fluids, distort the pattern of current flow and the electric field patterns in ways that can usually be recognized. Such dipole mapping surveys have been widely used in recent years in the search foe geothermal fields.

The areas surveyed are indicated on Figure 1, a sketch map of the Island of Hawaii. The Kilauea shield area was selected as the primary area for reconnaisance because a number of factors favor the occurence of geothermal heat in that area. A major consideration in assessing the favorability of Kilauea Volcano as a target for geothermal exploration is the high level of volcanic activity it has exhibited during recorded history. In addition, a number of wells have been drilled which have encountered shallow thermal waters with temperatures ranging from 30° to 100° C. along the northeast rift zone of Kilauea. Finally, the relatively low altitude at which the activity of Kilauea Volcano takes place is a favorable

GROUP SEVEN

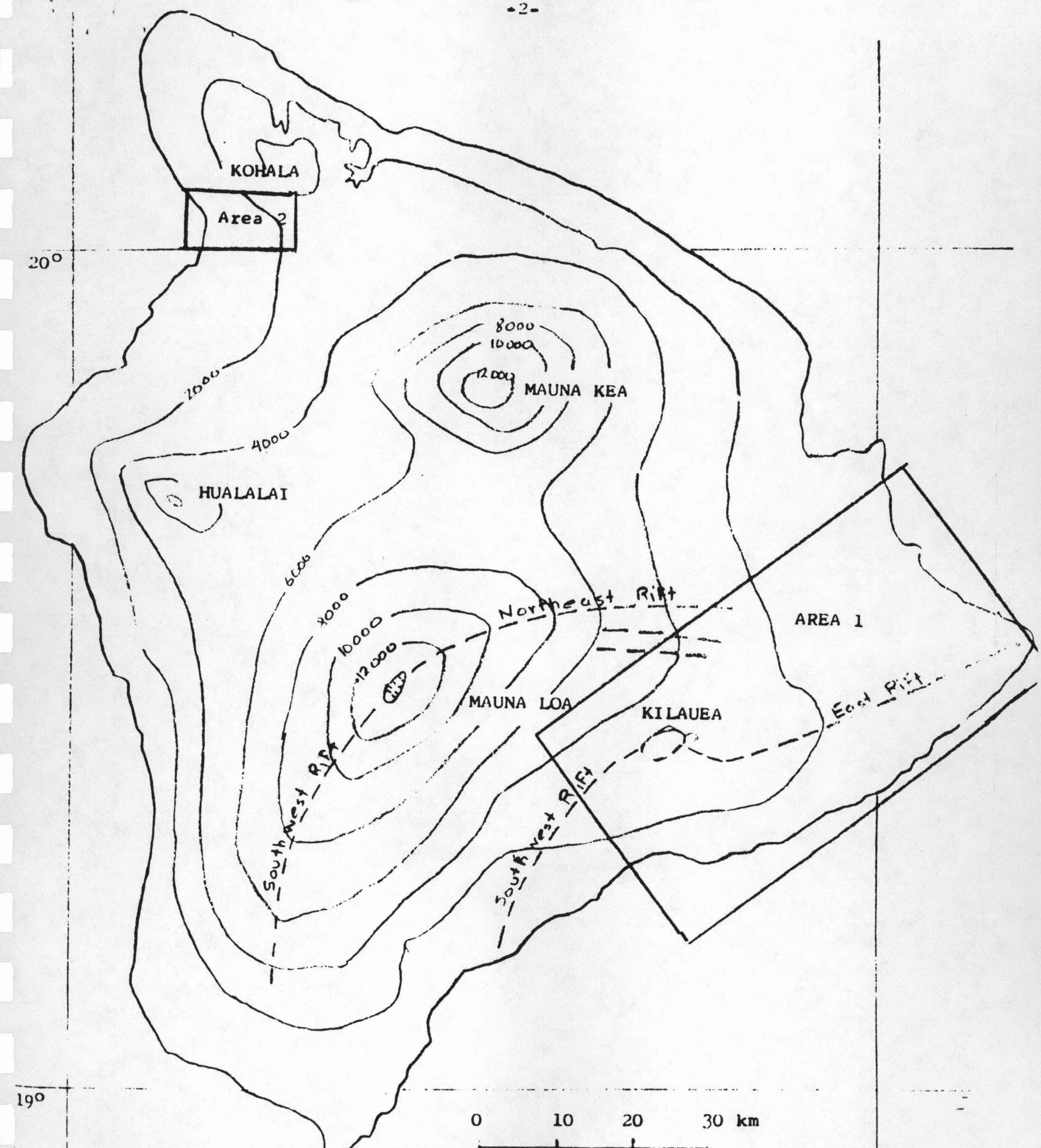

Figure 1. Map of the County of Hawaii showing the areas where electrical surveys were carried out. Area 1 covers the Kilauea shield in the Kau and Puna districts, while area 2 is in the South Kohala district. Elevation contours are in feet.

factor in terms of the ease with which geothermal fluids might be brought to the surface.

The details of the techniques used, the results obtained during the surveys, and a preliminary evaluation of the meaning of the data are included in the following sections of this report.

DESCRIPTION OF THE DIPOLE MAPPING METHOD

In a dipole mapping survey, a large amount of current is caused to flow in the earth between electrode contacts sited in the general vicinity of the area to be investigated. As the current flows through the ground from this bipole source, the flow pattern will be governed in detail by variations in the resistivity of the ground to a depth comparable to the offset distance at which measurements are being made, or to the depth to basement rock with high resistivity, whichever is less. Because the bipole source is fixed in location while many measurements of electric field are made around it, any electrical non-uniformities near the source will affect all the measurements to about the same extent, and variations in the behavior of the electric field from observation point to observation point will be indicative of the electrical structure of the ground primarily in the vicinity of the measurement sites.

The general scheme of a dipole mapping survey is indicated in Figure 2. For the surveys carried out on the island of Hawaii, 14 different source locations were used. Most of the source bipole lengths were approximately three kilometers, but in one case in which a pre-existing bipole was used (source 4), the length was 8 kilometers. Power was provided from a 15 KVA single-phase motor generator set. The 115-volt 60-Hz output was stepped up to 880 volts with a transformer, switched mechanically and rectified to form direct-current steps. A period of reversal of 18 seconds was used to assure that there would be time for the current to penetrate to the maximum depth possible during each current step. The current switches were operated at unequal intervals so that the current pulses were non-symmetrical, with current flow in one direction was about 30 percent longer in duration than current flow in the opposite direction. This non-symmetry permitted determination of the polarity of the electric field at the receiver site.

Some problems were encountered in obtaining ground contacts which would permit the use of the high currents normally required in dipole mapping surveys. The recent surficial lavas which cover almost the entire Puna and Kau districts have an extraordinarily high resistivity, so that even large-area electrodes planted at the surface have a high resistance. In cases where existing metal structures such as well casings or raod culverts could be used for grounds, such structures were used and good grounding was obtained. In a few areas where it became necessary to site bipole sources, no such structures were available, and in their place, lengths of metal pipe were buried in shallow trenches to serve as electrodes. With forty feet of pipe in a trench, wet down with salt water, a grounding resistance of 100 ohms could be obtained.

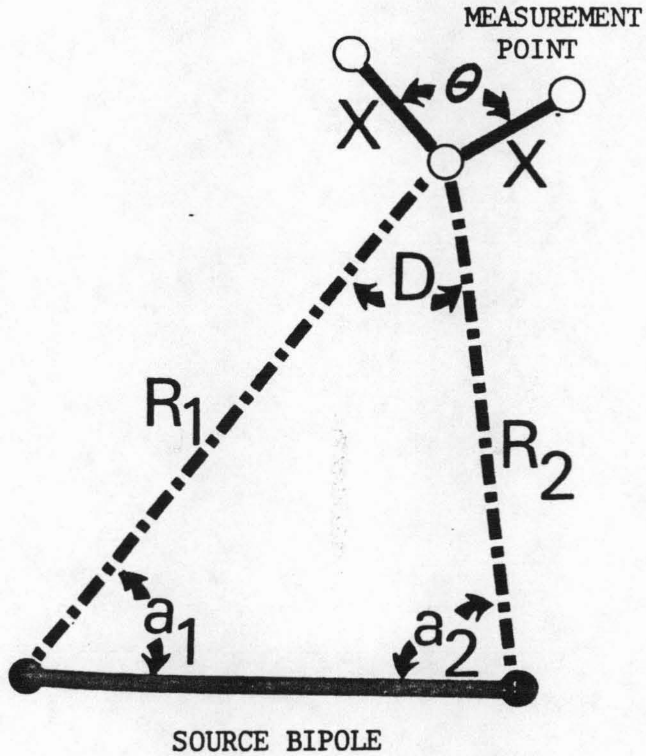

Figure 2. Layout of electrodes for a dipole mapping survey.

Amplitudes of current steps which were used ranged from as low as 1 to 2 amperes in a few cases in which it proved to be especially difficult to obtain a good ground contact to 10 to 20 amperes in the cases where existing metal structures were used for grounds. The amplitudes of the current steps were monitored visually with a meter and recorded.

The current field from a source bipole was mapped by recording the voltage drop between electrode pairs at many points around the source bipole. Because the direction of current flow at a measurement site is quite unpredictable, the total voltage drop must be determined by making a pair of measurements with electrode pairs oriented at right angles to one another and adding these voltages vectorially. Measurements were made with electrode separations of 30 to 300 meters, the larger separations being used in areas where the signal level was low. The receiving system consisted of a sensitive DC electrometer-voltmeter and recorder, on which the deflection of the trace was measured as the direction of current flow in the earth reversed. At the maximum sensitivity of the recorder, deflections as small as 5 microvolts can be recognized. An example of a record obtained with the recording system is shown in Figure 3.

The primary data obtained during the survey are listed in Tables 1-14, at the end of this report. These data may be converted to values of apparent resistivity using several different formulas. The conventional manner of defining apparent resistivity is to consider what resistivity a uniform earth would have to have to provide the voltages actually observed in the real earth. In a uniform earth, current spreads out from a single electrode with spherical symmetry. The electric field along the surface of the earth at a distance R_1 from a single electrode through which a current I is flowing is given by:

$$E_1 = \frac{\rho I}{2\pi R_1^2}$$

where ρ is the resistivity of the assumed uniform earth. When two source electrodes are used instead of one, there is a second contribution to the electric field from current flowing from the second electrode:

$$E_2 = \frac{-\rho I}{2\pi R_2^2}$$

where R_2 is the distance from the observation point to the second current electrode.

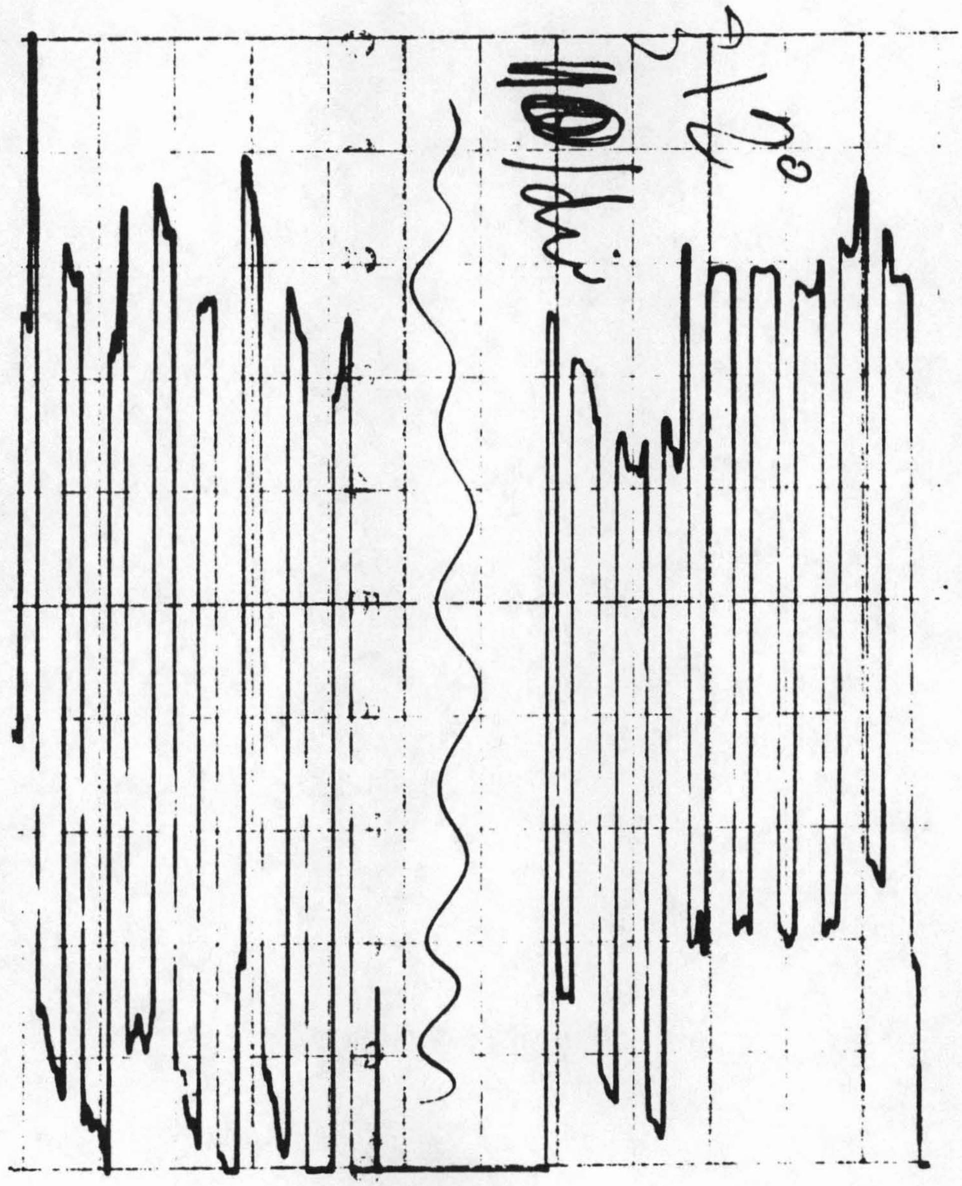

Figure 3. Example of a record of electric field components recorded at station 1434. Both components were recorded with a sensitivity of 10 microvolts per division. The component on the left was recorded along an azimuth of 52°, while the component on the right was measured along an azimuth of 312°. Electrode separation for both components was 30 meters.

The electric fields E_1 and E_2 are vector quantities, and so, must be added vectorially:

$$E_T = \frac{\rho I}{2\pi R_1^2}\left[1+\left(\frac{R_1}{R_2}\right)^4 -2\left(\frac{R_1}{R_2}\right)^2 \cos D\right]^{\frac{1}{2}}$$

Inversion of this equation to obtain an expression for ρ provides the definition of apparent resistivity used in dipole mapping. The expression for apparent resistivity is:

$$\rho_a = K_{g1}K_{g2}\frac{E}{I}$$

where $$K_{g1} = 2\pi R_1^2$$

and $$K_{g2} = \left[1 +\left(\frac{R_1}{R_2}\right)^4 - 2\left(\frac{R_1}{R_2}\right)^2\cos D\right]^{-1/2}$$

This formula is useful for doing computations in the field where a computer is not easily av ilable. The first geometric factor, K_{g1}, is exactly the Schlumberger array geometric factor if the distance R_1 is considered to be equivalent to half the current electrode separation in the Schlumberger array. The second geometric factor, K_{g2}, can be considered to be a correction which must be applied to the Schlumberger formula, and can be read from tables once the parameters R_1/R_2 and D have been scaled from the survey base map. A chart for determining the value for K_{g2} is shown in Figure 4.

In a real earth, the as umption of a uniform resistivity is not normally warranted. In geothermal exploration, a more realistic model in many cases is commonly that of a conductive section of rock resting on a high resistivity basement. In this case, the computation of apparent resistivity on the basis of assuming spherical spreading of current may not be appropriate. A more meaningful way to reduce the field data is to use a formula based on the assumption of cylindrical spreading of current in a thin conductive plate. For current spreading in a plate, the electric field depends on the ratio of plate thickness to resistivity, h/ρ, a quantity which is known also as the conductance of the plate, S. The electric field at the surface of the plate for a current I spreading from a single electrode is:

$$E_1 = \frac{I}{2\pi S R_1}$$

where R_1 is again the distance from the first current electrode tothe observation point. With the addition of a second elec-

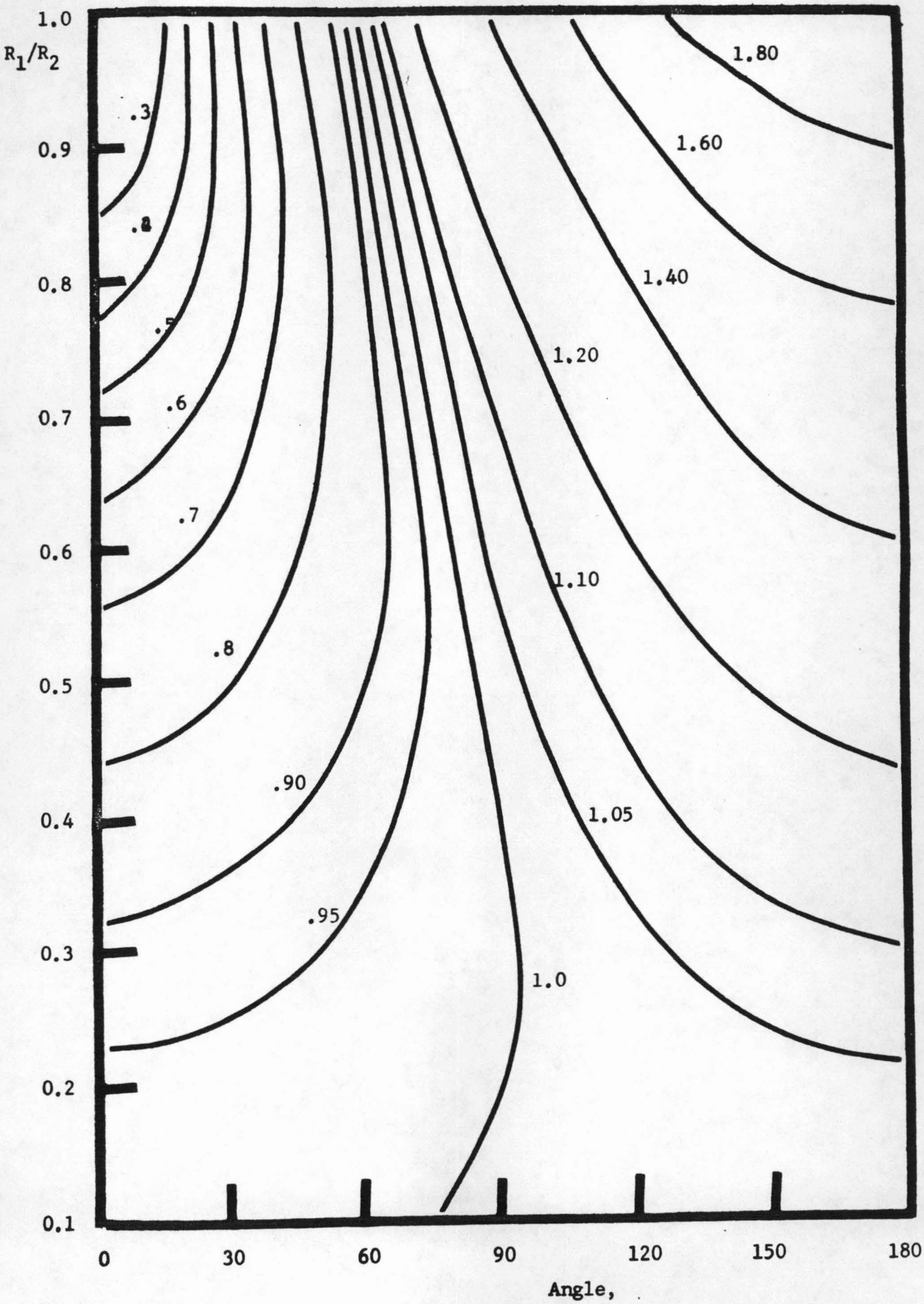

Chart of values for the geometric factor K trode to complete the bipole current source, the contribution of a second electric field at the observation point must be considered:

$$E_2 = \frac{-I}{2\pi SR_2}$$

The vector sum of these two electric fields is:

$$E_T = \frac{I}{2\pi SR_1}\left[1 + \left(\frac{R_1}{R_2}\right)^2 - 2\left(\frac{R}{R_2}\right)\right]\cos D^{\;1/2}$$

Solution of this equation for S provides the definition of "apparent conductance", S_a, under the assumption of cylindrical symmetry in the spreading of current through a uniform conducting plate.

Values were computed for both apparent resistivity and apparent conductance for all measurements made during this survey. It should be stressed that these are merely different forms for presentation of the same original data, rather than independent parameters. The choice of which to use is merely a matter of convenience, and depends on the character of the data which are acquired. The computed values are listed along with the primary data in Tables 1-14.

The apparent resistivity and apparent conductance maps obtained in a dipole mapping survey are useful primarily in reconnaisance, in looking for the boundaries of a conductive area such as may be associated with a hot-water-filled geothermal reservoir. In evaluation, one of the primary methods used is to compare the data obtained in the field survey with contour maps of data obtained in computer studies of hypothetical models. As a simple example of such a model study, a contour map of apparent resistivity for the case of a single conductive layer resting on an insulating basement structure is shown in Figure 5. The elliptical pattern on the apparent resistivity contours represents the increasing effect the resistant basement has on the measurements at larger distances from the source. If a geothermal reservoir were present and was characterized by a local area of low resistivity, these elliptical contours would be distorted. However, it must be recognized that the effect of basement provides an interference which makes it difficult to recognize the presence of local anomalies in resistivity, unless they are profound.

A contour map of apparent conductance values for the same case (Figure 6) illustrates the advantage of using apparent conductance values when the effect of a resistant basement structure is obvious in the data. Use of apparent conductance removes the strong tendency for contours to form

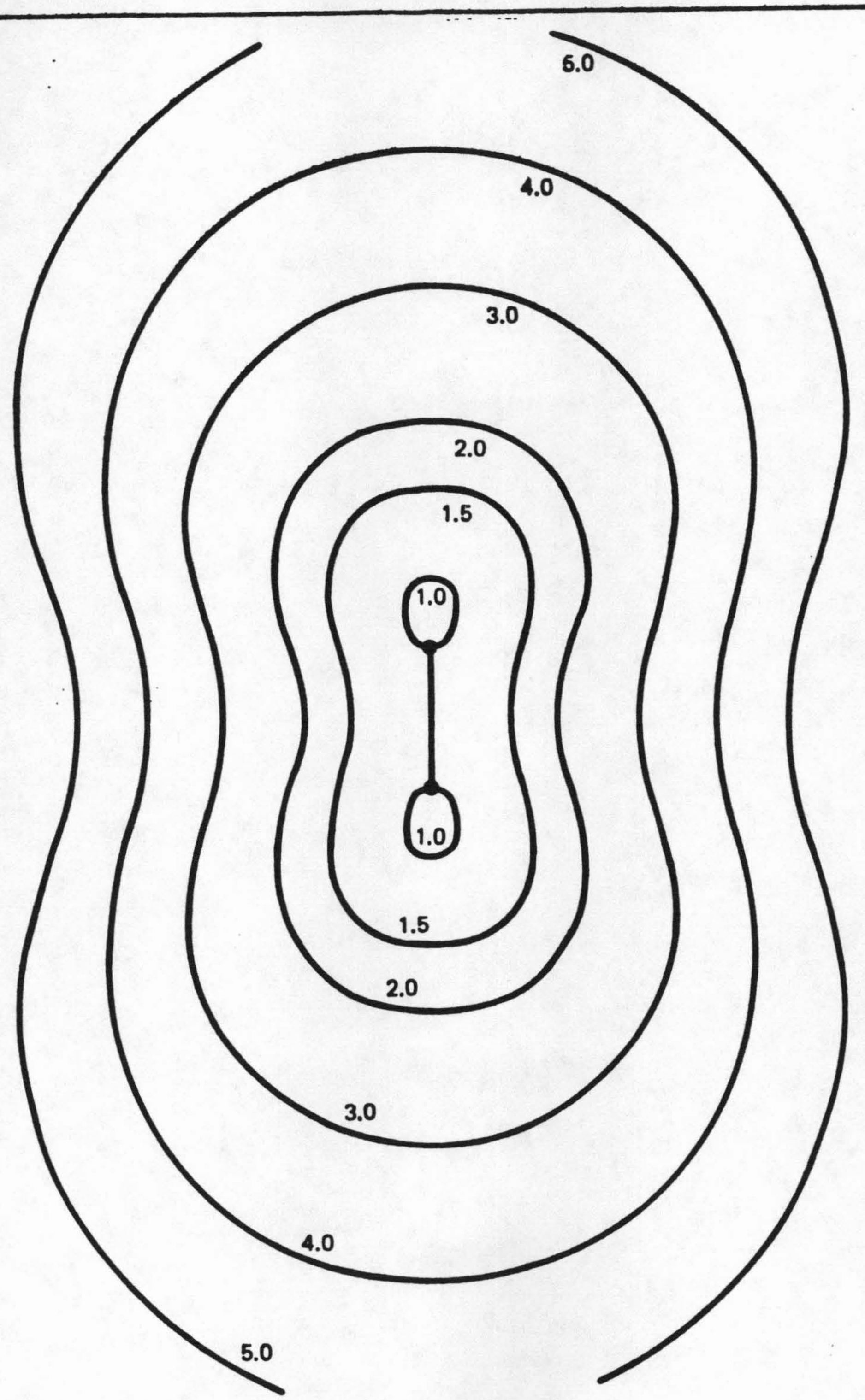

Figure 5. Apparent resistivity contours computed for the case of a conductive layer resting on an insulating substratum. The depth to the insulating layer is equal to half the source bipole length. Surface layer resistivity is unity.

GROUP SEVEN

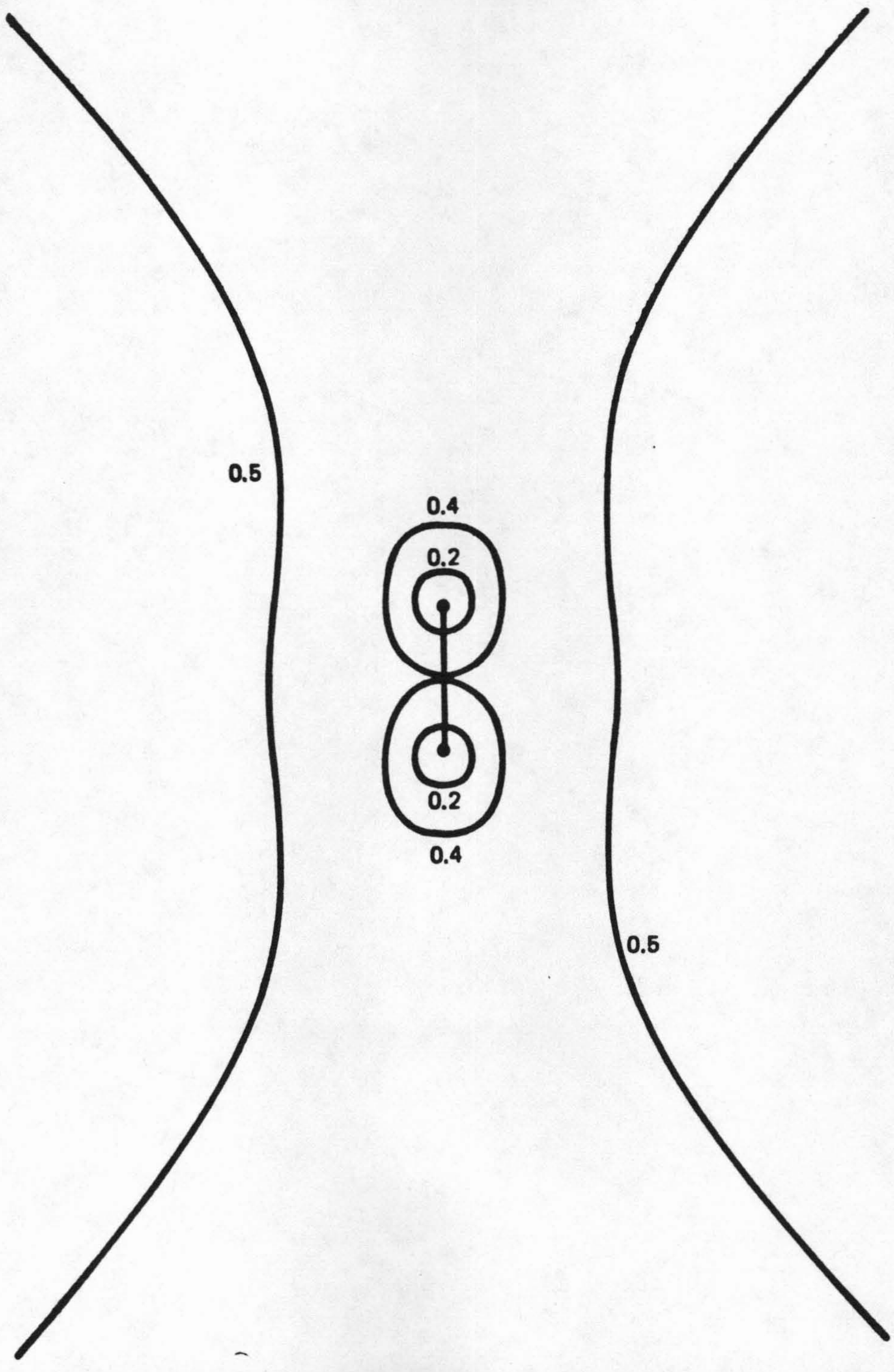

Figure 6. Apparent conductance contours computed for the case shown in Figure 5. Surface layer conductance is unity. If the depth to basement is made greater, both the contours shown here and the ones on Figure 5 will migrate outwards.

elliptical patterns. Without the elliptical tendency for the contours, it is somewhat easier to recognize local anomalies.

If the lower layer were more conductive than the surface layer, the apparent resistivities would again form an elliptical pattern about the bipole source, with the value of apparent resistivity decreasing rapidly at the greater distances from the source. It is possible to compute apparent conductance in this case, but the use of apparent conductance values is not advantageous because the conductance will increase even more rapidly with distance from the source than the rate at which inverse resistivity would increase. As a consequence, apparent conductance contours would provide an even more complicated elliptical pattern than would the apparent resistivity values, and in this case, it is necessary to use the apparent resistivities.

Normally, the information needed to choose between the two forms of presentation for the data are not known at the time the survey is carried out in the field. Whether the best mode of presentation is in terms of apparent resistivity or in terms of apparent conductance is usually determined by the overall behavior of the field data. A simple way of examining the data is to plot the apparent resistivity determinations for each bipole source as a function of the distance to the source (for standardization, the distance to the nearer end of the source is commonly used). Such a plot will show considerable scatter when there are lateral variations in the electrical properties of the ground present, but it will also commonly show the trend of resistivities with distance which reflects the variation of resistivity with depth in the earth. A summary of these trends for many of the bipole sources used in the Puna and Kau districts of the island of Hawaii is shown on Figure 7 (the complete plots for all these trend lines are contained in the next section of this report). It is clear that in many cases, the pres·nce of resistant rock at a depth of about 2 to 2-1/2 kilometers causes the data to exhibit the behavior which would warrant the use of apparent conductance values, at least for measurements made at distances greater than a few kilometers from the sources. However, many of the trend lines show a very large decrease in apparent resistivity with distance. These measurements weremade at higher elevations where the effect of resistant basement beneath the conductive zone is not evident even at the largest distances at which measurements were made. Inasmuch as it would be inappropriate to use apparent conductance maps for these cases, apparent resistivity maps were used for all bipole sources for consistency. However, the computed values of apparent conductance are included in Tables 1-14 in the event one would wish to make such a presentation.

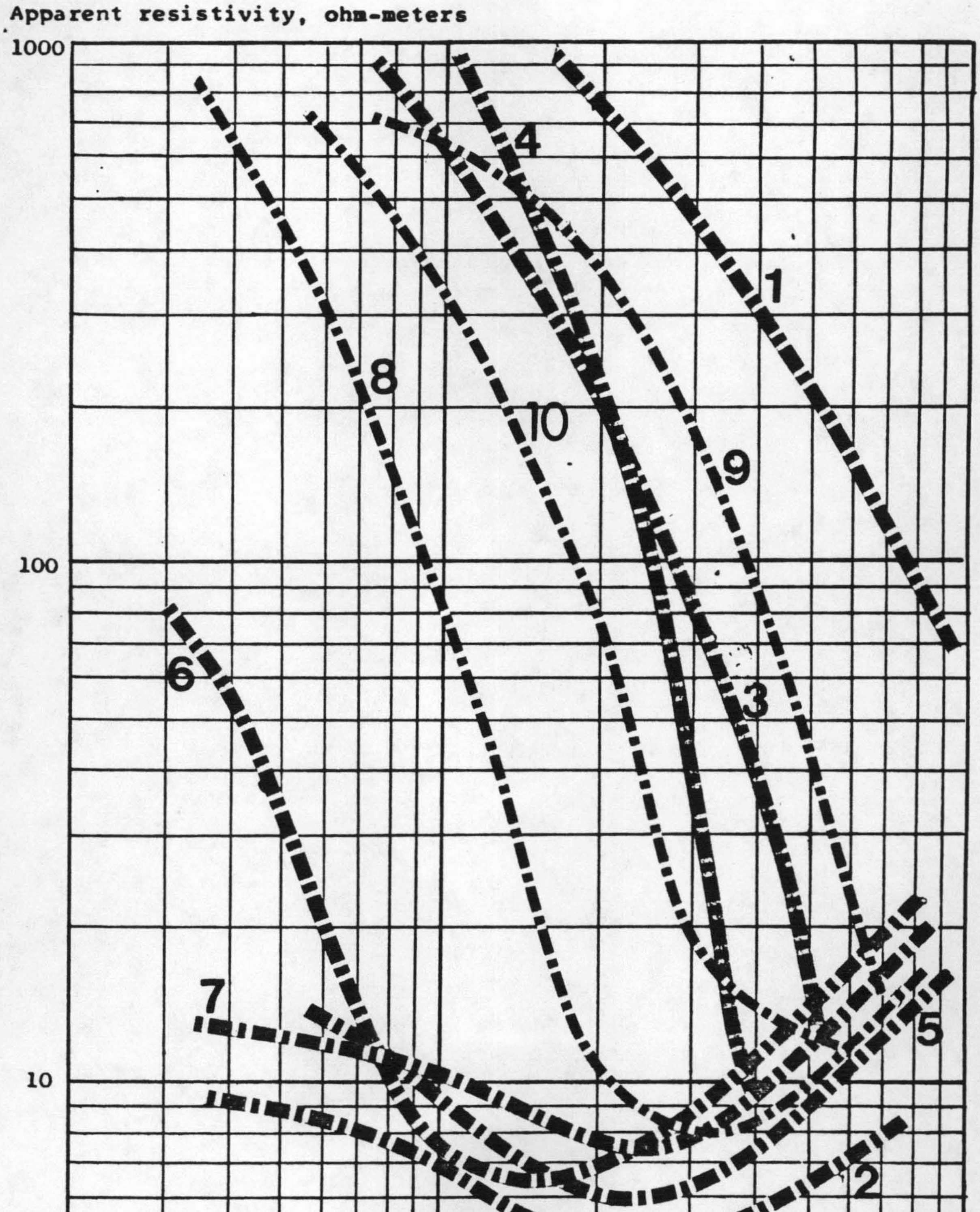

Figure 7. Trends of apparent resistivity values as a function of distance from the source.

1. Source 4, Mauna Loa side
2. Source 13, Pahoa side
3. Source 12
4. Source 11
5. Source 7
6. Source 8
7. Source 7, Kapoho side
8. Source 1
9. Source 3
10. Source 6

Ideally, one would wish to have the contours of apparent resistivity follow closely the boundaries of regions having different electrical characteristics, so that a non-ambiguous interpretation might be made merely by examining contour maps of apparent resistivity value. Unfor ately, this is rarely the case, being approximately true only when the dimensions of an anomalous area are small compared to the distance from the source, and then only if there are no other anomalous areas within range of the same source. In the case of linear boundaries between regions with different resistivities, the apparent resistivity contour patterns may vary radically, depending on the position of the source bipole with respect to the boundary. Because of this, when a boundary is located from one bipole source, it is higly advisable to examine the same boundary as illuminated with current from other bipole sources situated with a different aspect to the boundary. The reason for this may be seen by examining computer model studies for the simple case of a single vertical fault-like boundary.

Apparent resistivity contour maps are shown for the case of a single boundary separating two regions in which the resistivity varies by a factor of 10. The contour map in Figure 8 applies for the case in which the bipole source lies on the conductive side of the fault, while Figure 9 applies for the case in which the source lies on the resistive side of the fault. Considering Figure 8, we may see some of the patterns which make direct interpretation of dipole resistivity maps a bit uncertain:

1. There is apparently an area of anomalously low resistivity on the side of the fault facing the source bipole. This resistivity is lower than any real resistivity in the model by a factor of 2.

2. The resistivity on the far side on the fault is only sligthly higher than the resistivity on the near side, even though the true resistivies vary by a factor of 10.

These factors combine to make it possible for a resistive boundary such as a fault to be misinterpreted as being a local conductive feature if the area of low apparent resistivity is illuminated from only this one bipole source. If the anomalous area disappears or moves as the source is relocated, the reality of the anomaly must be suspect.

The behavior of the apparent resistivity contours is far less misleading if the source is located on the high resistivity side of the fault, as in Figure 9. Here, there are minor increases and decreases in apparent resistivity on the

Figure 8. Bipole resistivity map for a fault separating regions with tenfold contrast in resistivity.

	Y= 0.00	0.30	0.60	0.90	1.20	1.50	1.80	2.10	2.40	2.70	3.00
X= -1.6	0.10	0.10	0.10	0.10	0.10	0.10	0.10	0.10	0.10	0.10	0.10
X= -1.5	0.10	0.10	0.10	0.10	0.10	0.10	0.10	0.10	0.10	0.10	0.10
X= -1.4	0.10	0.10	0.10	0.10	0.10	0.10	0.10	0.10	0.10	0.10	0.10
X= -1.3	0.10	0.10	0.10	0.10	0.10	0.10	0.10	0.10	0.10	0.10	0.10
X= -1.2	0.10	0.10	0.10	0.10	0.10	0.10	0.10	0.10	0.10	0.10	0.10
X= -1.1	0.10	0.10	0.10	0.10	0.10	0.10	0.10	[illegible]	[illegible]	0.10	0.10
X= -1.0	0.10	0.10	0.10	0.10	0.10	[illegible]	0.10	0.10	0.10	0.10	0.10
X= -0.9	0.10	0.10	0.10	0.10	[illegible]	0.10	0.10	0.10	0.10	0.10	0.10
X= -0.8	0.10	0.10	0.12	0.11	0.10	0.10	0.10	0.10	0.10	0.10	0.10
X= -0.7	0.10	0.10	0.10	0.10	0.10	0.10	0.10	0.10	0.10	0.10	0.10
X= -0.6	0.10	0.10	0.10	0.10	0.12	0.10	0.10	0.10	0.10	0.12	0.10
X= -0.5	0.10	0.10	0.12	0.10	0.10	0.10	0.10	0.10	0.10	0.12	0.10
X= -0.4	0.10	0.10	[illegible]	0.10	0.10	0.10	0.10	0.10	0.10	0.12	0.10
X= -0.3	0.10	0.12	0.12	0.10	0.10	0.10	0.10	0.10	0.10	0.12	0.10
X= -0.2	0.10	0.12	0.10	0.10	0.10	0.10	0.12	0.10	0.10	0.10	0.12
X= -0.1	0.10	0.12	0.10	0.12	0.10	0.10	0.10	0.10	0.10	0.10	0.12
X= 0.0	[illegible]	[illegible]	0.10	0.10	0.12	0.10	0.10	0.10	0.12	0.10	0.10
X= 0.1	0.10	0.12	0.12	0.10	0.10	0.12	0.10	0.12	0.10	0.13	0.10
X= 0.2	0.10	0.12	0.12	0.10	0.10	0.10	0.10	0.10	0.10	0.12	0.10
X= 0.3	0.10	0.12	0.10	0.10	0.10	0.10	0.10	0.10	0.10	0.12	0.12
X= 0.4	0.10	0.12	0.12	0.10	0.10	0.10	0.10	0.10	0.10	0.10	0.12
X= 0.5	0.10	0.12	0.10	0.10	0.10	0.10	0.10	0.12	0.10	0.10	0.12
X= 0.6	0.10	0.12	0.10	0.10	0.10	0.10	0.10	0.10	0.10	0.12	0.12
X= 0.7	0.10	0.12	0.12	0.10	0.10	0.10	0.10	0.10	0.10	0.10	0.10
X= 0.8	0.10	0.12	0.12	0.10	0.10	0.10	0.10	0.10	0.10	0.10	0.10
X= 0.9	0.10	0.12	0.12	0.10	0.12	0.12	0.10	0.10	0.10	0.10	0.12
X= 1.0	0.13	0.12	[illegible]	0.10	0.10	0.10	0.10	0.10	0.10	0.10	0.09
X= 1.1	0.10	0.12	[illegible]	0.10	0.12	0.12	0.10	0.10	0.09	0.09	0.09
X= 1.2	0.10	0.12	[illegible]	0.10	0.10	0.10	0.10	0.10	0.09	0.09	0.09
X= 1.3	0.10	0.12	[illegible]	0.12	0.10	0.10	0.10	0.09	0.09	0.09	0.09
X= 1.4	0.10	0.12	0.12	0.10	0.10	0.10	0.09	0.09	0.09	0.09	0.09
X= 1.5	0.10	0.12	0.10	0.10	0.10	0.10	0.09	0.09	0.09	0.09	0.09
X= 1.6	0.10	0.12	0.12	0.10	0.10	0.09	0.09	0.09	0.09	0.09	0.09
X= 1.7	0.11	0.11	0.13	0.10	0.10	0.09	0.09	0.09	0.09	0.09	0.09
X= 1.8	0.11	0.11	0.12	0.10	0.12	0.09	0.09	0.09	0.09	0.09	0.09
X= 1.9	0.11	0.11	0.12	0.10	0.09	0.09	0.09	0.09	0.08	0.08	0.08
X= 2.0	0.11	0.11	0.12	0.13	0.09	0.09	0.09	0.08	0.08	0.08	0.08
X= 2.1	0.11	0.11	0.11	0.10	0.09	0.09	0.08	0.08	0.08	0.08	0.08
X= 2.2	0.12	0.11	0.11	[illegible]	0.09	0.09	0.08	0.08	0.08	0.08	0.08
X= 2.3	0.12	0.12	0.11	[illegible]	0.09	0.08	0.08	0.07	0.07	0.07	0.07
X= 2.4	0.13	0.12	0.11	[illegible]	0.09	0.08	0.07	0.07	0.07	0.07	0.07
X= 2.5	0.13	0.13	0.12	0.12	0.09	0.08	0.07	0.06	0.06	0.06	0.07
X= 2.6	0.14	0.13	0.12	0.10	0.09	0.07	0.06	[illegible]	[illegible]	0.06	0.07
X= 2.7	[illegible]	[illegible]	0.13	0.11	0.09	0.07	0.06	[illegible]	[illegible]	0.05	0.06
X= 2.8	0.16	[illegible]	0.13	0.11	0.09	0.07	[illegible]	0.04	0.04	[illegible]	0.06
X= 2.9	0.17	0.15	0.14	0.12	0.09	[illegible]	0.04	0.03	0.03	0.04	0.06
X= 3.0	[illegible]	[illegible]	[illegible]	[illegible]	[illegible]	[illegible]	[illegible]	[illegible]	[illegible]	[illegible]	[illegible]
X= 3.1	0.19	0.15	0.15	0.18	0.10	[illegible]	[illegible]	0.14	0.16	0.18	0.15
X= 3.2	0.19	0.15	0.19	0.18	0.14	[illegible]	0.15	0.15	0.10	0.16	0.15

Figure 9. Dipole sistivity map for a fault s rating regions with a tenfold contrast in resistivi

	Y= 0,00	0,30	0,60	0,90	1,20	1,50	1,80	2,10	2,40	2,70	3,00
X= -1,6	0,99	0,99	0,99	0,99	1,00	1,00	1,00	1,00	0,99	0,99	0,99
X= -1,5	0,99	0,99	0,99	1,00	1,00	1,00	1,00	1,00	1,00	1,00	0,99
X= -1,4	0,99	0,99	1,00	1,00	1,00	1,00	1,00	1,00	1,00	1,00	0,99
X= -1,3	0,99	1,00	1,00	1,00	1,00	1,00	1,00	1,00	1,00	1,00	1,00
X= -1,2	1,00	1,00	1,00	1,00	1,00	1,00	1,00	1,00	1,00	1,00	1,00
X= -1,1	1,00	1,00	1,00	1,00	1,00	1,00	1,00	1,00	1,00	1,00	1,00
X= -1,0	1,00	1,00	1,00	1,00	1,00	[illegible]	1,00	1,00	1,00	[illegible]	1,00
X= -0,9	1,00	1,00	1,00	1,00	[illegible]	1,00	1,00	1,00	1,00	1,00	1,00
X= -0,8	1,00	1,00	1,00	1,00	1,00	1,00	1,00	1,00	1,00	1,03	1,00
X= -0,7	1,00	1,00	1,00	[illegible]	1,00	1,00	1,00	1,00	1,00	1,02	1,00
X= -0,6	1,00	1,00	1,00	1,00	1,00	1,00	1,00	1,00	1,00	1,03	1,00
X= -0,5	1,00	1,00	1,00	1,00	1,00	1,00	1,00	1,00	1,01	1,01	1,01
X= -0,4	1,00	1,00	[illegible]	1,00	1,00	1,00	1,00	1,01	1,01	1,01	1,01
X= -0,3	1,00	1,00	[illegible]	1,00	1,00	1,00	1,00	1,01	1,01	1,01	1,01
X= -0,2	1,00	1,00	[illegible]	1,00	1,00	1,00	1,00	1,01	1,01	1,01	1,01
X= -0,1	1,00	1,00	1,00	1,00	1,00	1,00	1,01	1,01	1,01	1,01	1,01
X= 0,0	[illegible]	[illegible]	1,00	1,00	1,00	1,00	1,01	1,01	1,01	1,01	1,02
X= 0,1	1,00	1,00	1,00	1,00	1,00	1,00	1,01	1,01	1,01	1,02	1,02
X= 0,2	1,00	1,00	1,00	1,00	1,00	1,01	1,01	1,01	1,02	1,02	1,02
X= 0,3	1,00	1,00	1,00	1,00	1,00	1,01	1,01	1,01	1,02	1,02	1,02
X= 0,4	1,00	1,00	1,00	1,00	1,00	1,01	1,01	1,02	1,02	1,02	1,03
X= 0,5	1,00	1,00	[illegible]	1,00	1,00	1,01	1,01	1,02	1,02	1,03	1,03
X= 0,6	1,00	1,00	[illegible]	1,00	1,01	1,01	1,01	1,02	1,03	1,03	1,03
X= 0,7	1,00	1,00	[illegible]	1,00	1,01	1,01	1,02	1,02	1,03	1,03	1,04
X= 0,8	1,00	1,00	[illegible]	1,00	1,01	1,01	1,02	1,03	1,03	1,04	1,04
X= 0,9	0,99	1,00	[illegible]	1,00	1,01	1,02	1,02	1,03	1,04	1,05	1,05
X= 1,0	0,99	0,99	[illegible]	1,01	1,01	1,02	1,03	1,04	1,04	1,05	1,06
X= 1,1	0,99	0,99	[illegible]	1,01	1,01	1,02	1,03	1,04	1,05	1,06	1,06
X= 1,2	0,98	0,99	[illegible]	1,01	1,02	1,03	1,04	1,05	1,06	1,07	1,07
X= 1,3	0,98	0,98	1,00	1,01	1,02	1,03	1,05	1,06	1,07	1,08	1,08
X= 1,4	0,97	0,98	1,00	1,01	1,03	1,04	1,05	1,07	1,08	1,09	1,09
X= 1,5	0,97	0,97	0,99	1,01	1,03	1,05	1,06	1,08	1,09	1,10	1,11
X= 1,6	0,96	0,97	0,99	1,01	1,04	1,06	1,08	1,09	1,10	1,11	1,12
X= 1,7	0,94	0,95	0,99	1,02	1,04	1,07	1,09	1,11	1,12	1,13	1,14
X= 1,8	0,93	0,94	0,98	1,02	1,05	1,08	1,10	1,12	1,14	1,15	1,16
X= 1,9	0,91	0,93	0,97	1,02	1,06	1,10	1,12	1,15	1,16	1,17	1,18
X= 2,0	0,89	0,91	0,97	1,02	1,07	1,11	1,15	1,17	1,19	1,20	1,20
X= 2,1	0,86	0,89	0,96	1,03	1,09	1,14	1,17	1,20	1,22	1,23	1,23
X= 2,2	0,83	0,87	0,95	1,03	1,11	1,16	1,20	1,23	1,25	1,26	1,26
X= 2,3	0,80	0,84	0,94	1,04	1,13	1,19	1,24	1,27	1,29	1,30	1,32
X= 2,4	0,75	0,82	0,92	1,05	1,16	1,23	1,28	1,32	1,34	1,34	1,34
X= 2,5	0,69	0,75	0,91	1,07	1,19	1,28	1,34	1,37	1,39	1,39	1,39
X= 2,6	0,63	0,71	0,97	1,09	1,23	1,33	1,42	1,44	1,45	1,45	1,44
X= 2,7	0,54	0,65	[illegible]	1,12	1,29	1,42	1,47	1,51	1,52	1,52	[illegible]
X= 2,8	[illegible]	0,62	[illegible]	1,16	1,36	[illegible]	1,56	1,60	1,61	1,59	1,57
X= 2,9	0,33	0,36	[illegible]	1,23	[illegible]	1,59	1,66	1,70	1,70	1,69	1,65
X= 3,0	[illegible]	[illegible]	[illegible]	[illegible]	[illegible]	[illegible]	[illegible]	[illegible]	[illegible]	[illegible]	[illegible]
X= 3,1	0,18	[illegible]	0,18	0,18	0,18	0,18	0,18	0,18	0,18	0,18	0,18
-	[illegible]	[illegible]	[illegible]	0,18	0,18	0,18	0,18	0,18	0,18	0,18	0,18

side of the fault facing the source, but the major change in apparent resistivity is the decrease that is observed in crossing the fault. From this, it should be concluded that more definitive results are obtained in dipole mapping when a conductive region is illuminated using a source located outside the conductive area than in the inverse case. This is further apparent from profiles of apparent resistivity which might be observed along traverses crossing the boundary (Figures 10 and 11). In Figure 10, such profiles are shown for two orientations of the source bipole, one perpendicular to the boundary (the upper curve), and one parallel to the boundary (the lower curve) for the case in which the source is located in the conductive region. As may be seen, the jump in apparent resistivity is only by a factor of 1.8 at the boundary, rather than by the actual factor of 10. Moreover, if the source is parallel to the boundary, a small area of very low resistivity appears on the side of the fault facing the source. On the other hand, if the source is located on the resistive side of the fault, as for the curves in Figure 11, the effect of the fault on the measurements is profound and unmistakable. However, even in this case, the contrast in apparent resistivity on crossing the fault is less than the contrast in actual resistivities.

Many more complicated models may be used for computer studies related to interpretation of dipole mapping surveys. However, these few examples are adequate to explain the various strategies used in carrying out the survey of the Puna and Kau districts of the Island of Hawaii. Although 14 sources were used, each covering an area of 50 to 100 square miles, considerable overlapping coverage was provided in two areas where anomalously low resistivity features were recognized. Because of this overlapping coverage, a total area of approximately 600 square miles was covered by the surveys described in this report.

The data obtained from the individual dipole sources are described in the next section of this report.

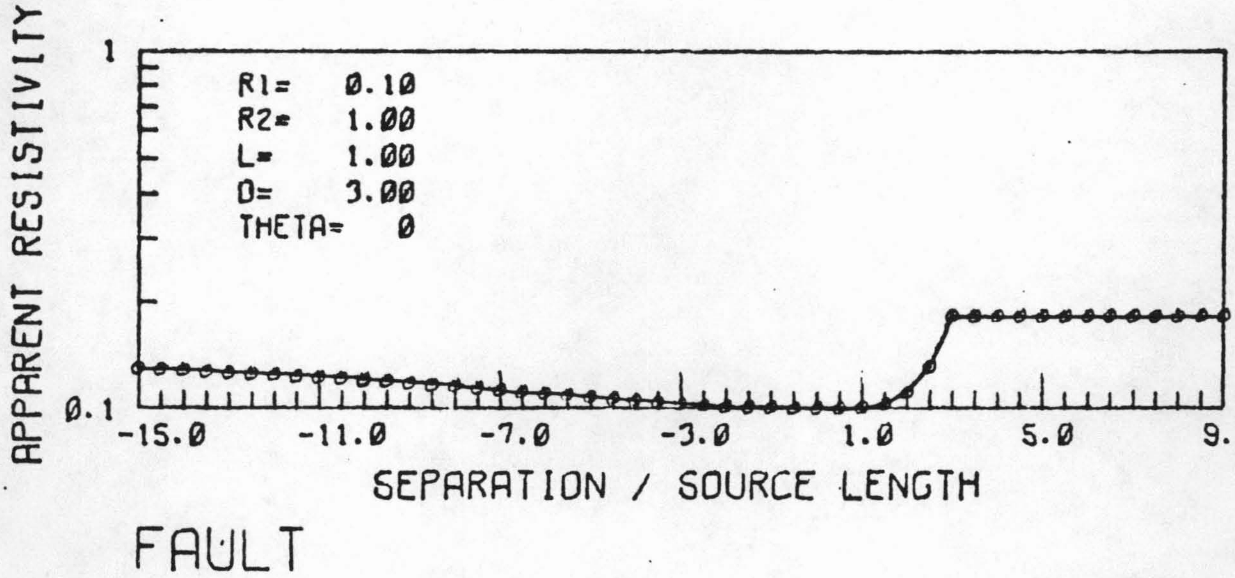

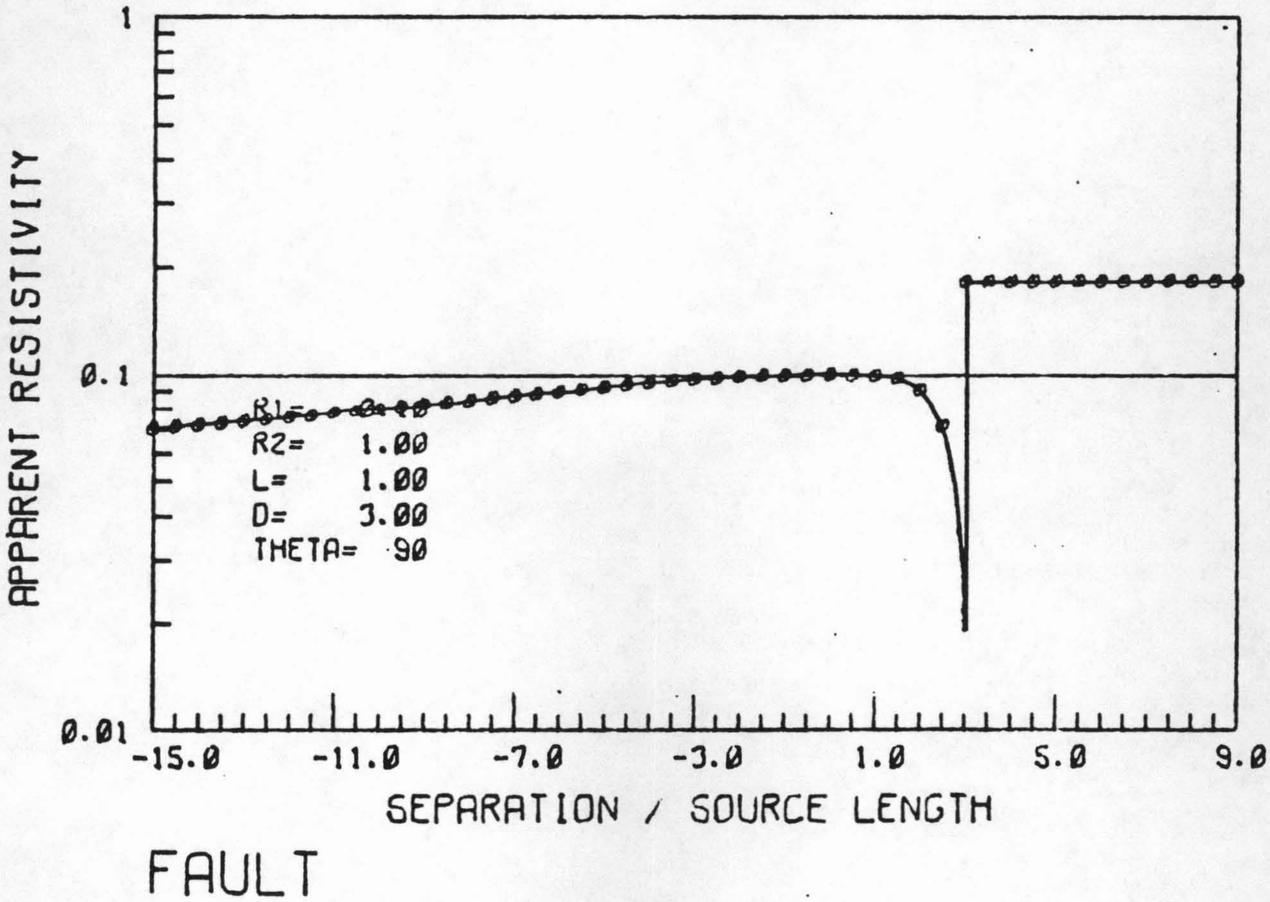

Figure 10. Apparent resistivity profiles for traverses crossing a fault that separates two regions with tenfold different resistivities. The source is located on the conductive side of the fault. The upper profile applies for the case in which the source is perpendicular to the fault, while the lower profile applies to the case in which the source is parallel

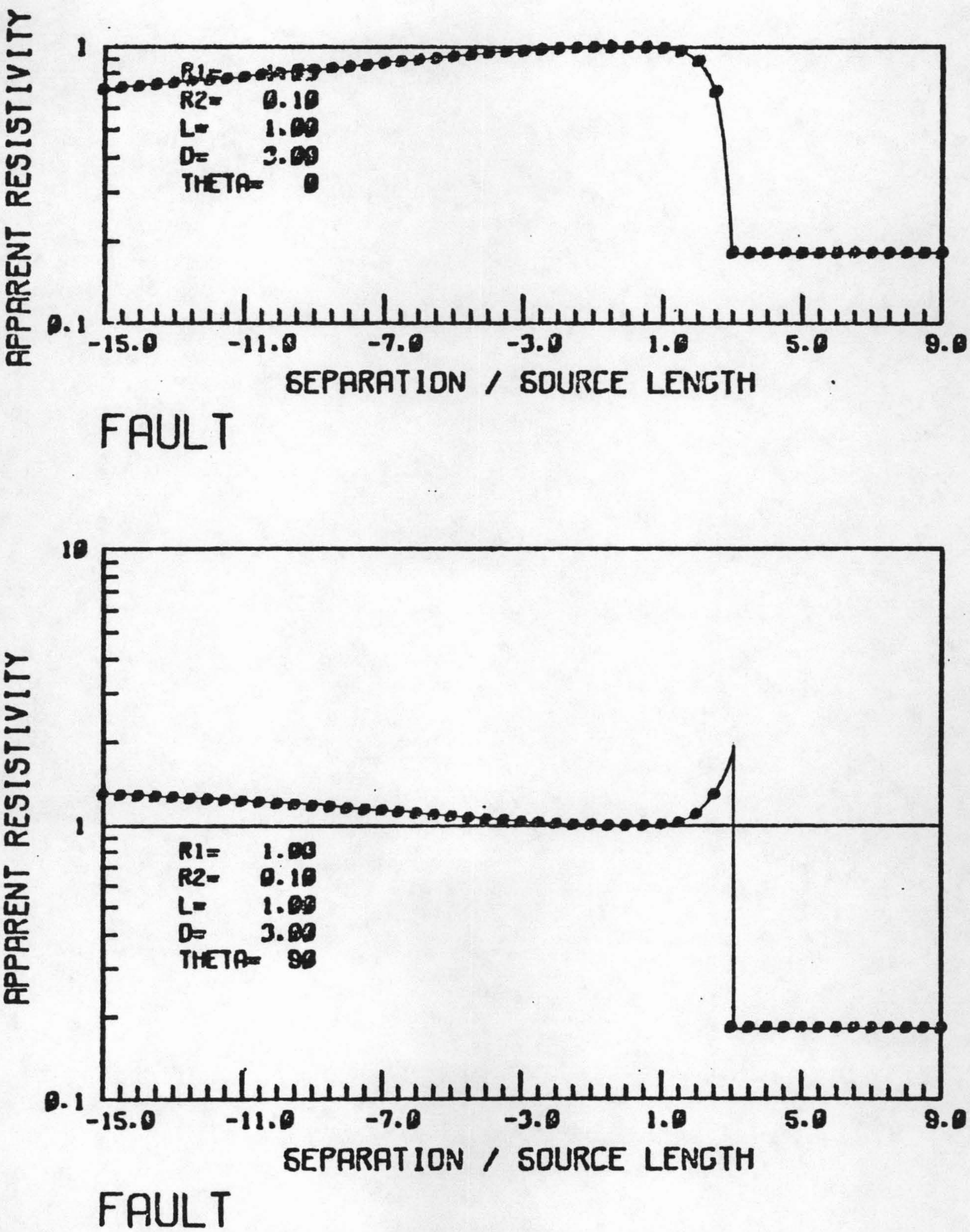

Figure 11. Apparent resistivity profiles for traverses crossing a fault that separates two regions with tenfold different resistivities. The source is located on the resistive side of the fault. The upper profile applies for the case in which the source is perpendicular to the fault, while the lower profile applies in the case in which the source is parallel.

RESULTS FROM DIPOLE MAPPING SURVEYS

Thirteen bipole sources were used in mapping resistivity over the Kilauea shield area in the Puna and Kau districts, and one additional source was used for measurements between Kamuela and Kawaihae, in the district of South Kohala. The results are shown in this section of the report in the form of apparent resistivity contour maps and plots of values of apparent resistivity as a function of distance from the source. Because values of apparent resistivity determined at a single receiver station using several different bipole sources may be radically different, it is not usually possible to present overlapping coverage of an area on a single basemap. Therefore, the results will be presented here as contour maps of apparent resistivity for each bipole source individually. These results are presented on basemaps at a scale of 1:62 500 prepared from U. S. Geological survey topographic maps of the area, printed at a scale of 1:24 000. Each of the individual maps covers an area of 7 by 9 miles; for some bipole sources, two such maps are necessary to cover the entire area surveyed. The boundaries of these small maps are indicated on a larger map covering the entire survey area in the Puna and Kau districts, included as Plate I with this report.

In preparing the resistivity contour maps, a geometric progression of contoured intervals is used, rather than making the contours equally spaced; that is, the contour levels used are 2.5, 5, 10, 20, 40, 80, 150, 320, etc., ohm-meters. It might also be noted that considerable difficulties were caused by the presence of power lines along some of the major raods in the survey area. These power lines contained a neutral conductor which was grounded at intervals of a half mile or so. This grounded neutral conductor served to redistribute current which would normally flow in the ground in such a manner as to cause a high resistivity anomaly along the power lines and for a distance of up to a quarter mile on either side of the line. In contouring the data, these features are confusing, and should not be considered as being significant in terms of earth electrical structures.

Source 3.

Bipole source 3 was located along the Volcano highway, in the vicinity of Glenwood. The source was grounded at both ends using highway culverts. Because of the relatively high current that was obtained, and because of the high apparent resistivities which were measured, a considerable area was covered using this source. The resistivity contour maps are shown in two parts, on Figures 15A and 15B. The first of these covers the area uphill from the source, toward Kilauea Volcano, while the second covers the area downhill from the source, towards Hilo. The most impressive feature of the measurements made from this source is the generally high level of apparent resistivity. However, there appear to be boundaries separating this area of high resistivity from areas of lower resistivity both in the direction towards Kilauea Caldera and towards Hilo.

Two plots of apparent resistivity as a function of distance are included in Figures 16 and 17. The first of these was based on measurements made in the uphill direction. These data form a pattern which can be interpreted as indicating the presence of a surface layer with a resistivity of about 700 ohm-meters extending to a depth of about 3.2 kilometers. This layer is underlain by rock with a resistivity of about 15 ohm-meters, though even the measurements made at a distance of 10 kilometers from the source are not sufficiently far from the source to provide a definitive value for the second-layer resistivity.

Measurements made in the downhill direction from this source show very much the same behavior, except that the depth to conductive rocks appears to be even greater, in the range from 3.5 to 4 kilometers. There is a strong possibility that no conductive rocks underly the area about the Glenwood source, and that the decrease in apparent resistivity with distance represents a lateral change in resistivity.

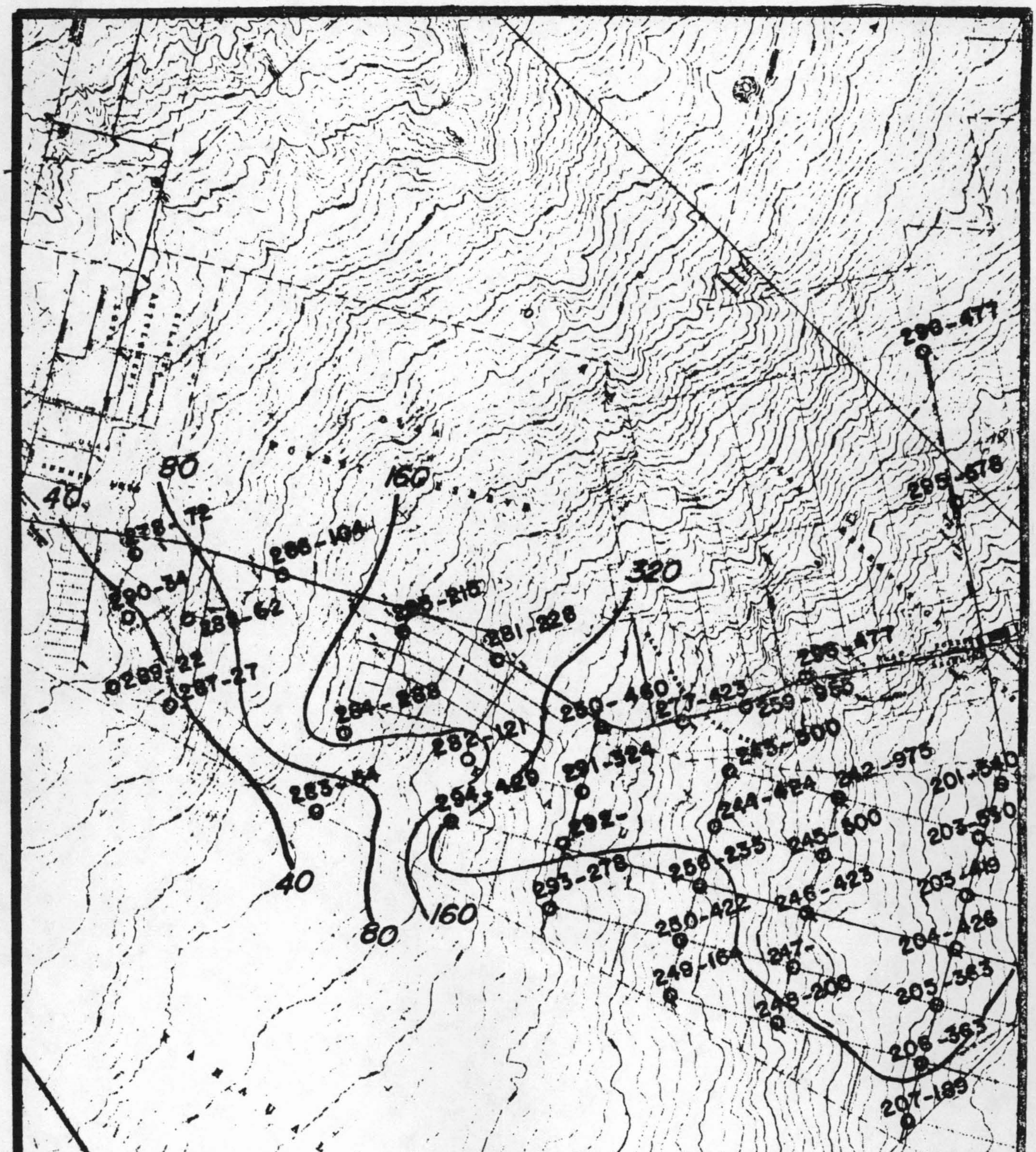

Figure 15A. Apparent resistivity map for measurements made in the direction of Kilauea Volcano from the source 3, located at Glenwood on the Volcano highway.

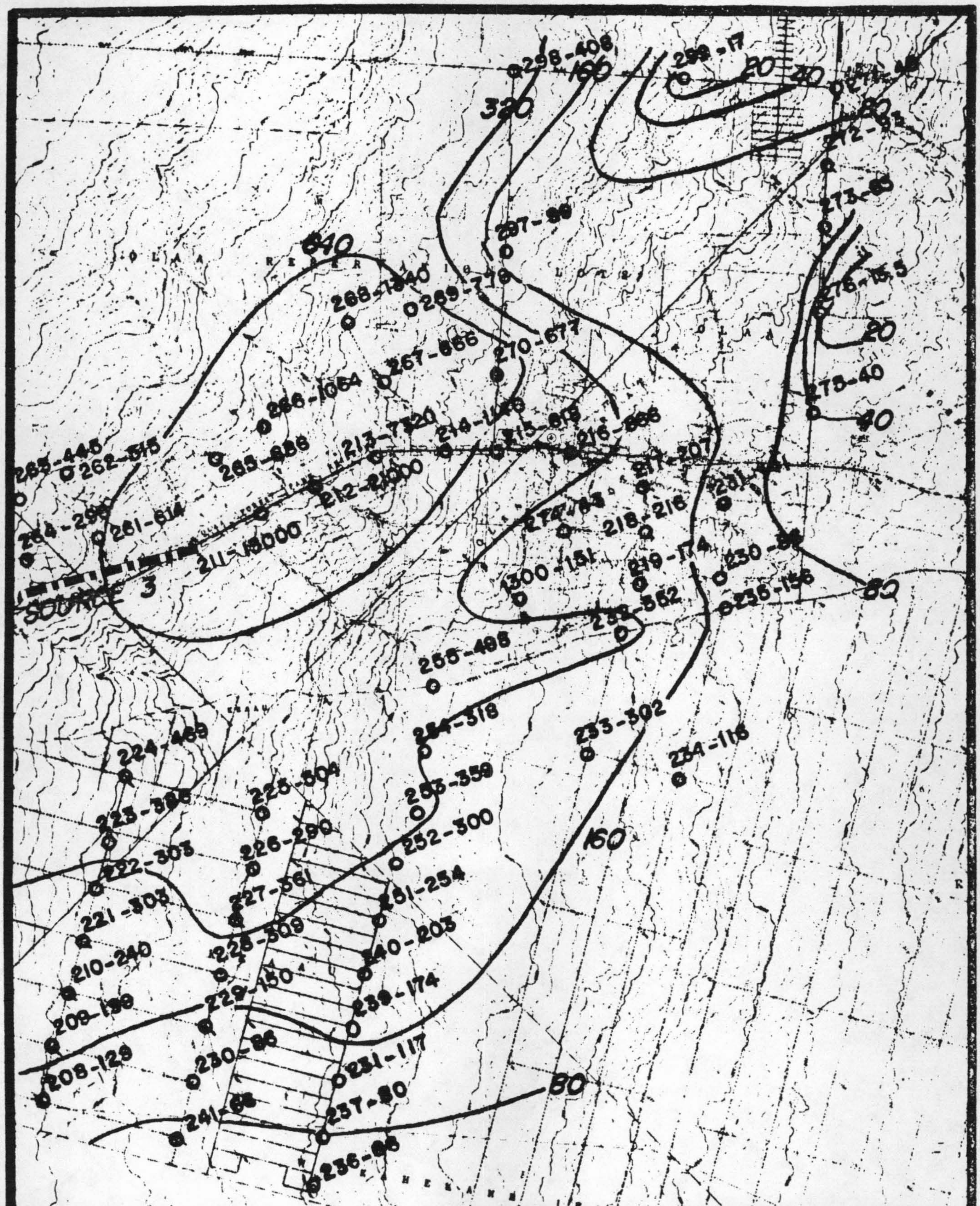

Figure 15B. Apparent resistivity map for measurements made in the direction of Hilo and Puna from source 3, located at Glenwood on the Volcano highway.

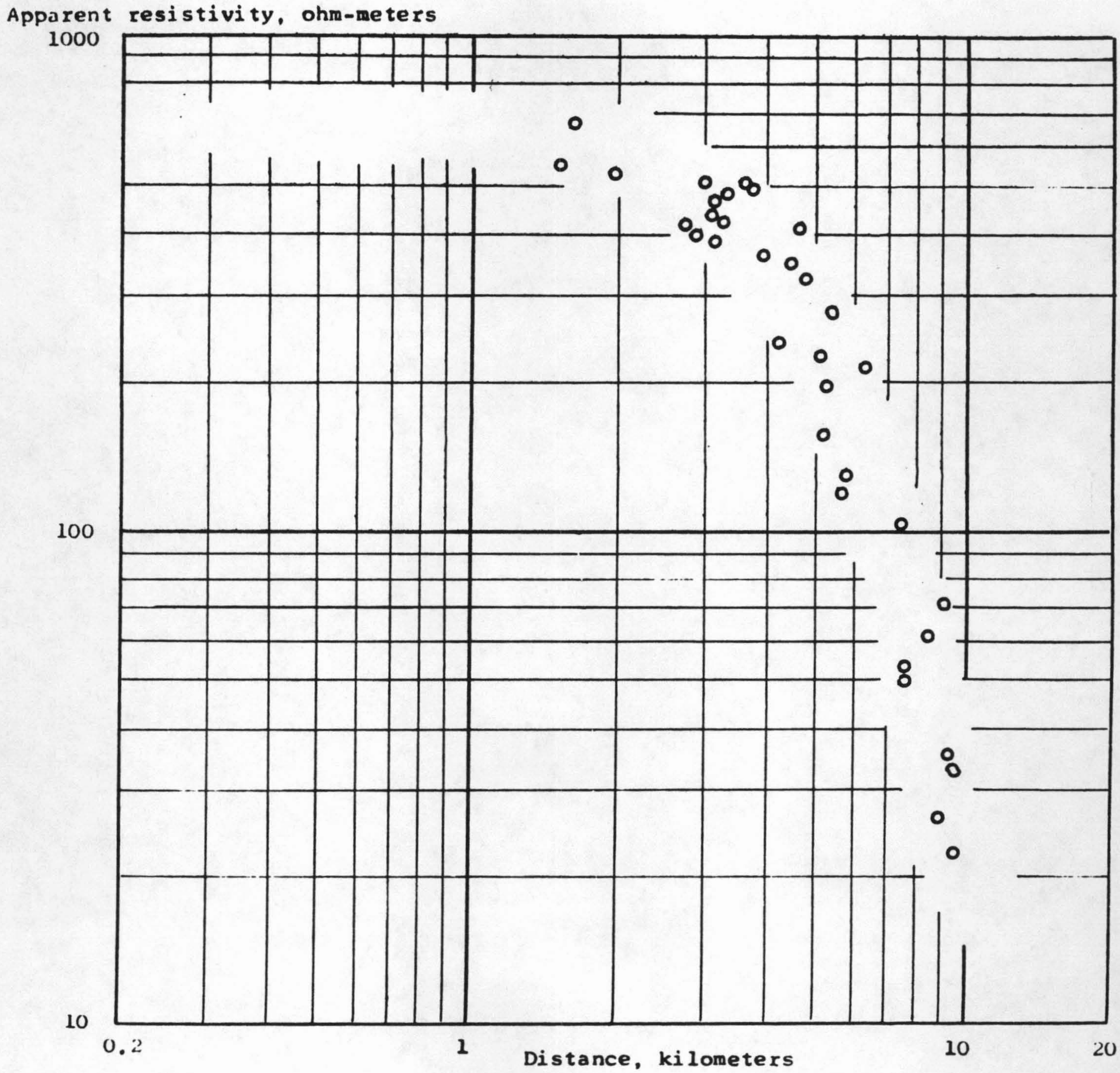

Figure 16. Apparent resistivity values measured in the direction toward Kilauea Volcano from source 3 at Glenwood plotted as a function of distance.

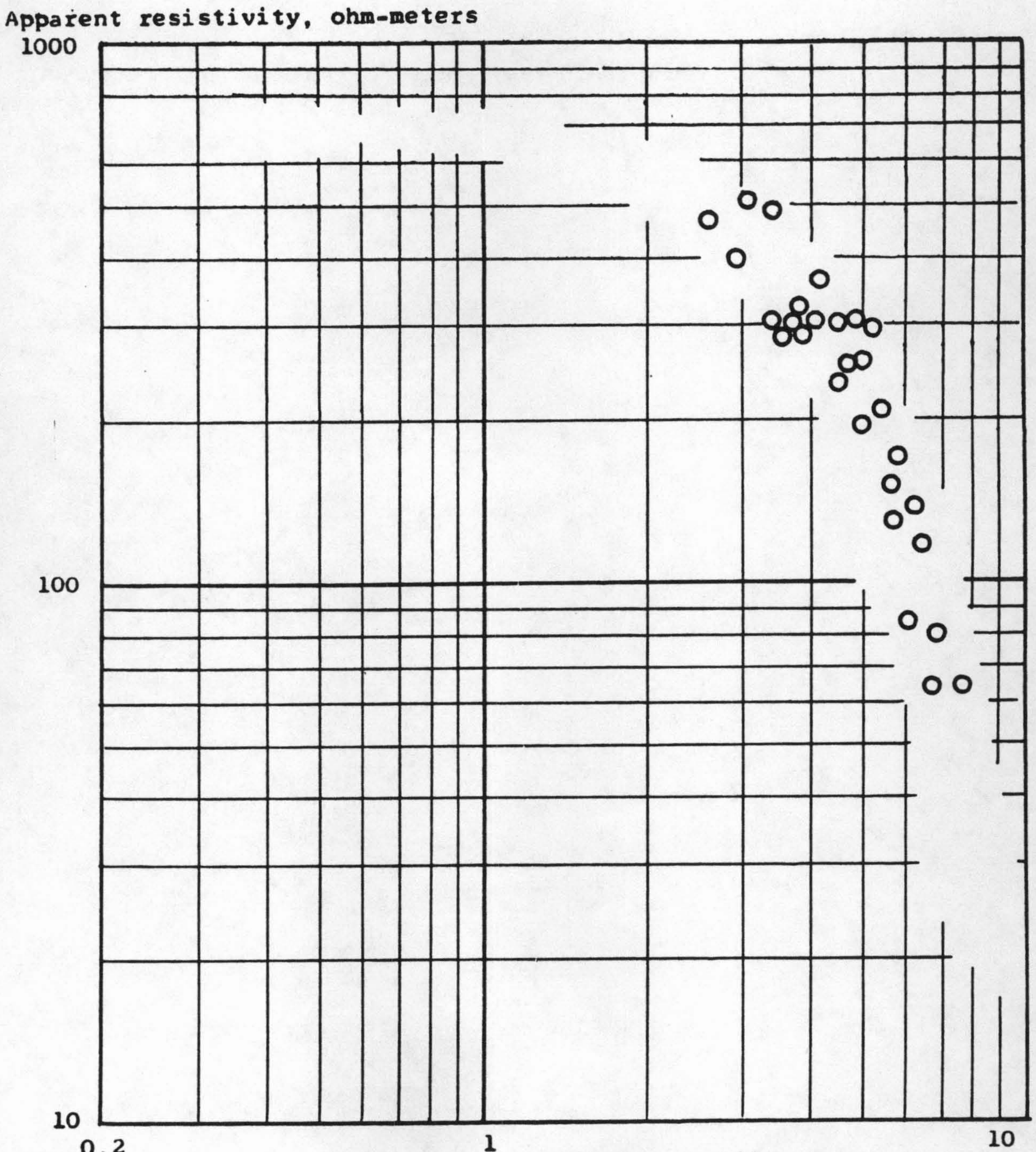

Figure 17. Apparent resistivity values measured in the direction toward Hilo and Puna from source 3 at Glenwood as a function of distance.

Source 6.

Bipole source 6 was located along the Escape Road, which parallels the upper East Rift of Kilauea within the Hawaii Volcanoes National Park. It was located to examine the possible extension of the low resistivity area under Kilauea Crater to the east near Kilauea Iki or along the East Rift. Ground contacts were made using lengths of buried pipe, but grounding resistance was very high. Only limited measurements could be made from this source. The apparent resistivities measured from this source are shown in Figure 24. A strong elliptical pattern for the resistivity contours is apparent. No particularly low resistivity values were measured in the target areas for this dipole.

A plot of apparent resistivity as a function of distance is shown in Figure 25. These data indicate a very high surface resistivity, greater than several thousand ohm-meters, probably extending to a depth of 1. to 1.3 kilometers. The resistivity at greater depths is probably between 10 and 20 ohm-meters, though measurements could not be made at a great enough distance to provide a definitive value.

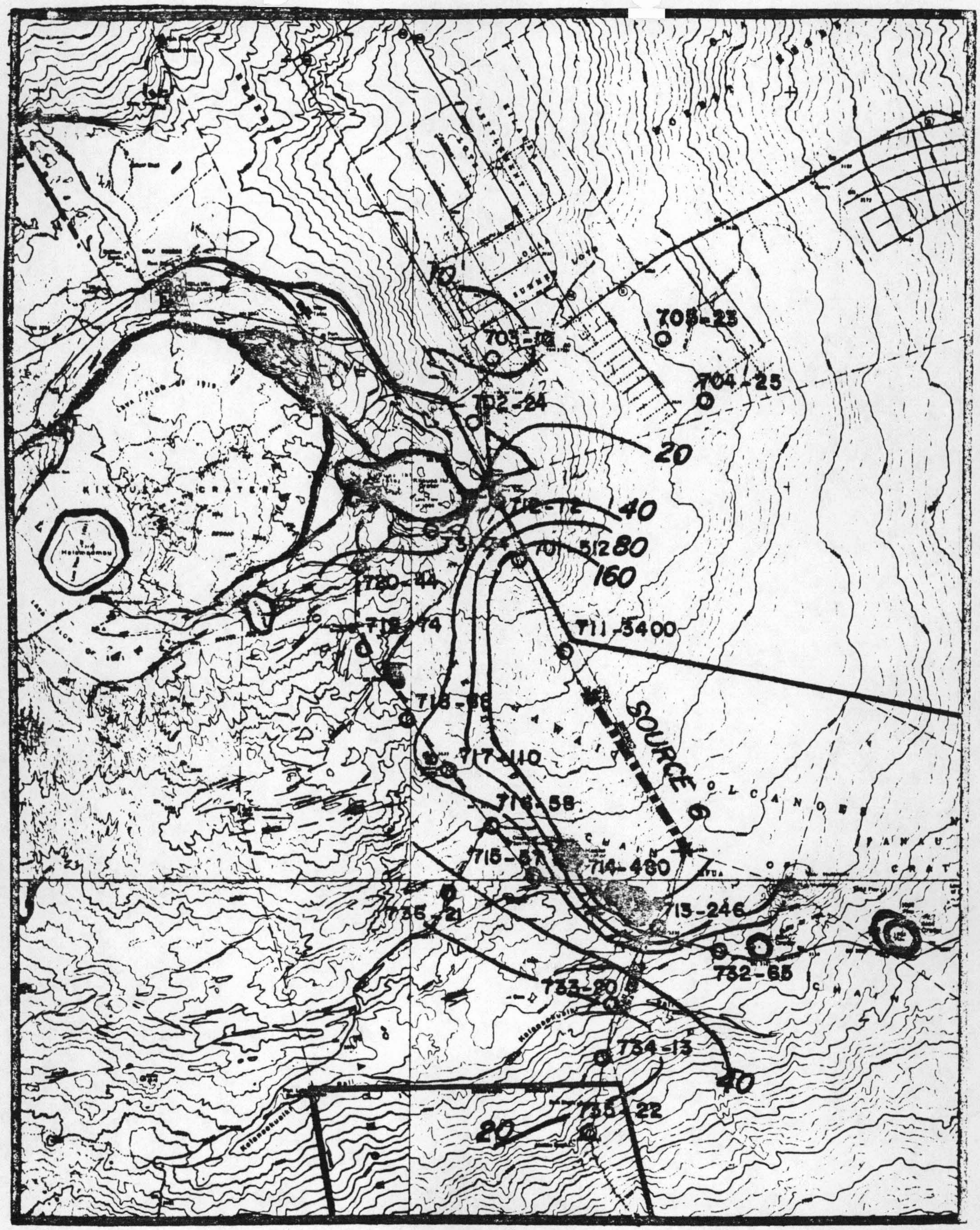

Figure 24. Apparent resistivities measured from source 6, located along the Escape Road in the Hawaii Volcanoes National Park.

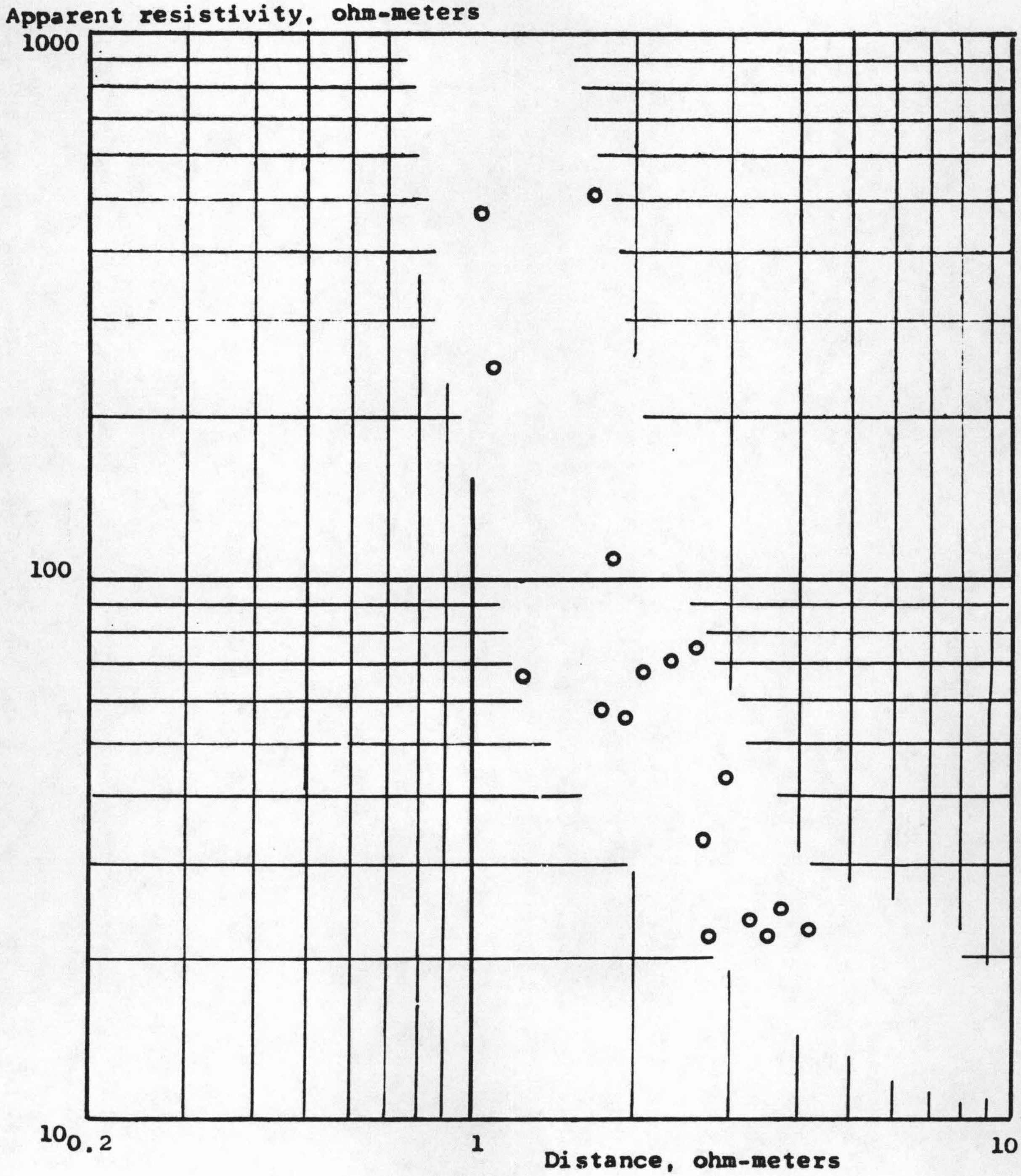

Figure 25. Apparent resistivities measured from source 6 plotted as a function of distance.

Source 9.

Bipole source 9 was located along a back road paralleling the East Rift of Kilauea several miles inland from Kalapana. Buried pipe was used for ground contacts at both ends of the source, and only limited current could be obtained. This source was sited to illuminate the low resistivity zone in the Kaimu-Kehena area from outside the low resistivity zone. The apparent resistivities are shown in Figure 31. Quite high resistivities were measured from the southwest end of this source; the boundary to the low resistivity area that was thetarget for this source appears to lie along the Kaimu-Pahoa road. No plot of the apparent resistivity as a function of distance is included because of the strong lateral changes in resistivity apparent from these data.

Figure 31. Apparent resistivities measured from bipole source 9, located inland from Kalapana.

Source 11.

Bipole source 11 was located in the village of Twenty-nine Mile, just outside the north entrance of Hawaii Volcanoes National Park. It was sited to illuminate a possible area of low resistivity in the vicninity of Kilauea Iki and the upper East Rift of Kilauea Volcano. Contacts were made thorugh lengths of pipe buried in the ground. Only a small amount of current was obtained, which limited the area that could be covered from this source. The apparent resistivities are shown on Figure 33. High resistivities were observed near the source. There is a rapid gradient in resistivity in going into the Kilauea Caldera area, as had been noted in measurements made from sources 3 and 4. No particularly low values were noted around Kilauea Iki or along the upper East Rift. This is surprising, in view of the current activity along the East Rift.

A plot of the apparent resistivities measured from source 11 as a function of distance from the source is shown in Figure 34. The behavior is almost identical with that seen from source 6, which was located along the Escape Road. Surface rocks have a very high resistivity, greater than 1000 ohm-meters, to a depth of about 1.5 kilometers. These are underlain by rocks with a resistivity of 10 to 20 ohm-meters, though measurements could not be made at great enough distances to provide a definitive value for the resistivity at depth.

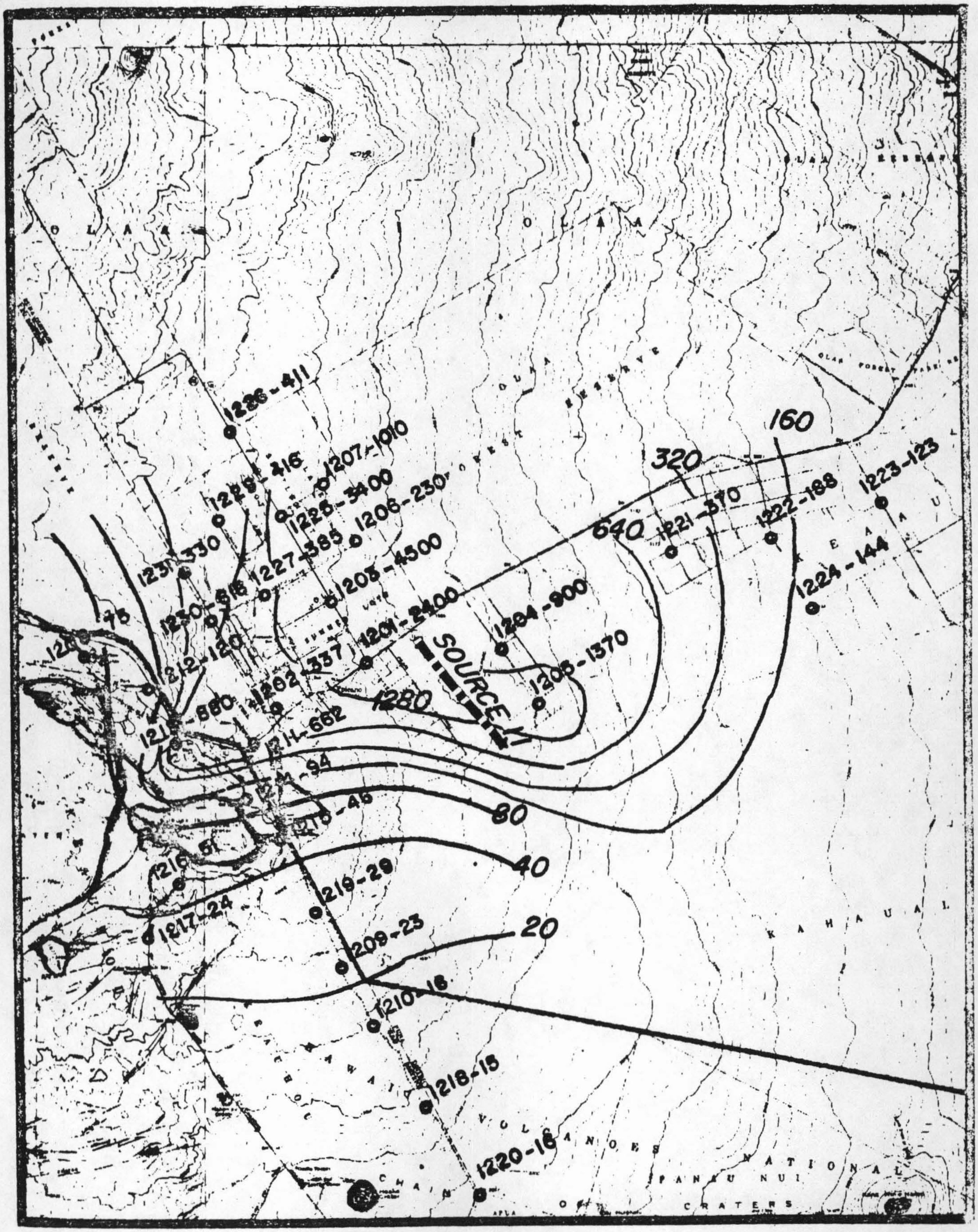

Figure 33. Apparent resistivities measured from source 11, near the north entrance to Hawaii Volcanoes National Park.

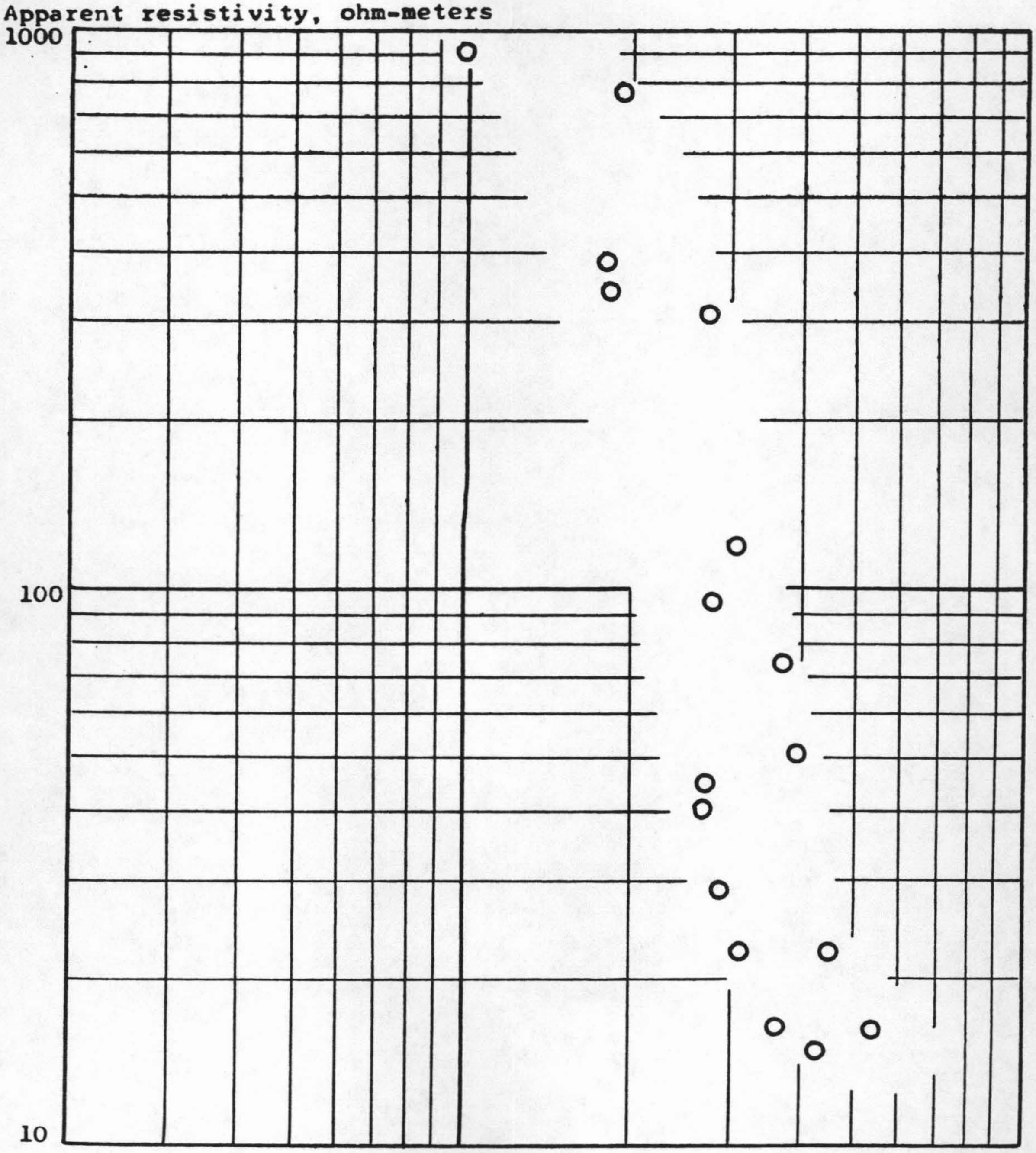

Figure 34. Apparent resistivities measured from source 11, plotted as a function of distance from the source.

RESULTS FROM RESISTIVITY SECTIONING SURVEYS

Dipole mapping surveys are useful primarily as a reconnaisance exploration technique for locating areas of anomalously low resistivity such as might be associated with geothermal reservoirs. However, the resolution with which the boundaries may be located is poor, and very little information is obtained about the variation of resistivity with depth. Once a prospective area has been located, it is advisable to carry out detailed studies to obtain such information, using both electrical sounding methods and other geophysical techniques. While detailed surveys were not a large part of the work described in this report, some resistivity sectioning was done in the vicinity of the low resistivity areas in Puna to estimate the depths to the tops of the conductive zones.

The resistivity sectioning technique used here was the pole-dipole method; other methods which might have been used equally well are the dipole-dipole and Schlumberger sectioning methods. The pole-dipole technique was used here because it required no change in instrumentation and virtually no change in field procedures. In the pole-dipole method, a bipole source two kilometers long was used. The electric field component in line with the bipole source was measured at intervals of 100 meters along a traverse extending from either end of the bipole source, from a closest distance of 150 meters to a farthest distance of 1250 meters. Values of apparent resistivity were computed in exactly the same way as was used for the dipole mapping results.

The term "resistivity sectioning" arises because of the manner in which the results from such surveys are presented. A section is prepared using the horizontal location of a measurement as the horizontal position at which a value is plotted, and by using the distance from the end, or "pole", of the source as a vertical coordinate. The purpose is to suggest that the distance that a measurement is made from a pole is equivalent to the depth at which the resistivity is determined. This is not precisely true, but the resulting presentation resembles a resistivity vs depth section in many respects.

Resistivity sectioning was done along the road from Pahoa to Kaimu, and along the Hilo-side edge of the East Rift near Kapoho Crater. The locations are shown on Plate III, along with a summary of the other resistivity data. The resistivity sections are shown on Plate IV.

The resistivity sectioning done along the Pahoa-Kaimu road shows the presence of a narrow zone of low resistivity in the

Vicinity of the geothermal well drilled in the early sixties. This is also the location at which the surface trace of the East Rift crosses the Pahoa-Kaimu road. The lowest values of resistivity are somewhat less than 25 ohm-meters, not as low as the lowest values seen with the dipole mapping survey in this area. However, it must be remembered that the resistivity sectioning survey provides considerably less penetration than does the dipole mapping survey. With a maximum spacing of 1250 meters, the apparent resistivities measured here are related largely to rocks within the first 600 meters of the surface.

A single setup was used to obtain sectioning data at locations offset seaward from the low resistivity zone seen on the Pahoa-Kaimusection (see point 5 on Plate IV). Lower resistivities, near 5 ohm-meters, were observed at the larger offset distances at which measurements were made. It appears that the depth to the conductive rock at this location is only about 600 meters.

Even lower apparent resistivities were measured along the section by Kapoho Crater (locations 4 and 6, Plate IV). The lowest resistivities were recorded from the north end of setup 6, with apparent resistivities of 5 ohm-meters or less being recorded for all spacings beyond 450 meters. This indicates that the surface layer of high resistivity is only a few tens of meters thick at most, and that at depths beyond 1000 meters, the resistivity is probably less than 2 ohm-meters.

SUMMARY AND EVALUATION

The important feautures of the individual dipole resistivity maps are summarized on a basemap on Plate III. Perhaps the most significant feature shown by the resistivity surveys is the contrast between the areas underlain by high resistivity material to the north of Kilauea Caldera and extending into the Puna area east of Mountain View, and reaching into the vicinity of Pahoa, and the surrounding areas of lower resistivity. Because this zone of high resistivity geographically coincides with the eastward extension of the Northeast Rift Zone of Mauna Loa under the recent Kilauea lavas, it is reasonable to assume that these high resistivities are associated with a Mauna Loa dike complex.

This area of high resistivity is probably not of interest for exploration for a geothermal reservoir. A typical geothermal reservoir would be characterized by a relatively high porosity and, if it is to be used readily for electrical power generation, a temperature in excess of 180° C. Both factors will cause a rock to have a lower resistivity than might otherwise be the case. Thus, in prospecting for a geothermal reservoi, we search for a region with diagnostically low values of electrical resistivity.

Sufficient information is available about the way in which resistivity depends on other physical parameters to allow us to specify the limits of observed resistivity which may be required to provide a basis for recognizing the presence of a worthwhile geothermal reservoir. The electrical resistivity of a water-bearing rock is determined by the amount of the water contained in the pore spaces of the rock, the resistivity of that water, and to some extent, the way in which the water is distributed through the rock. This relationship has been determined experimentally for many types of rocks, with the results being as shown graphically in Figure 39. For a specific rock type, and over a limited range in porosity, relationships such as those shown in Figure 39 can be described by a simple algebraic expression:

$$F = \rho/\rho_w = a\,\phi^{-m}$$

where F is defined as the resistivity formation factor of a rock (a useful and widely used parameter for describing the electrical behavior of a rock), ρ is the bulk resistivity of a rock completely saturated with water having a resistivity ρ_w, ϕ is the volume fraction of the rock filled with water (the porosity if the rock is fully saturated with water), and a and m are experimentally determined parameters. These parameters,

GROUP SEVEN

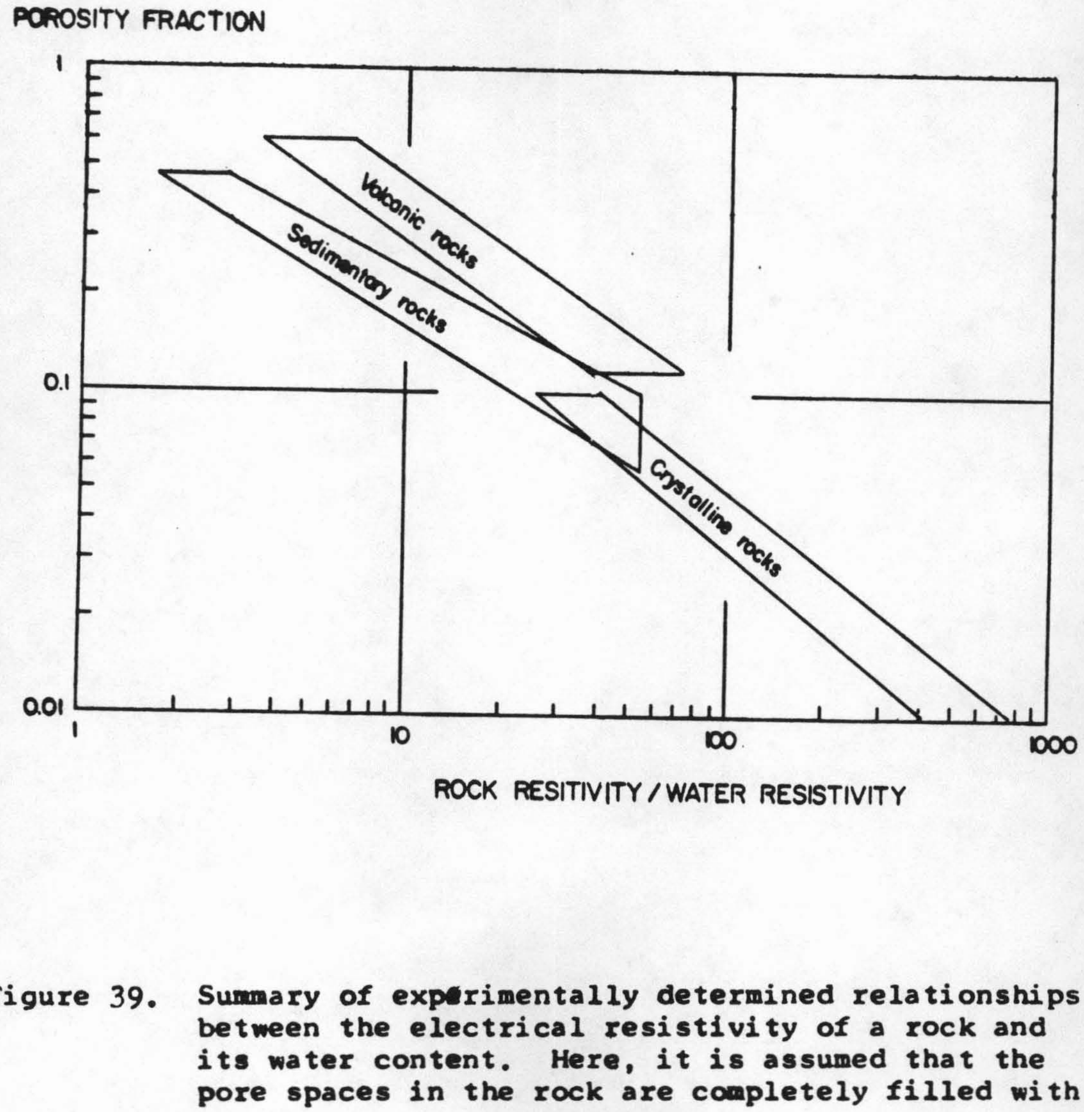

Figure 39. Summary of experimentally determined relationships between the electrical resistivity of a rock and its water content. Here, it is assumed that the pore spaces in the rock are completely filled with water.

a and m, are determined by making measurements of resistivity, water resistivity, and water content on a large number of small rock samples, and then fitting such an algebraic relationship to the data so obtained. Such a procedure has been employed for a number of samples of Kilauea flows on the surface, with the results as shown in Figure 40. The large degree of scatter is typical of determinations of porosity and resistivity made on small samples, with volumes of 10 to 20 cc. It is generally assumed that the scatter will decrease to insignificant levels if measurements can be made on large enough samples are used so that statistical variations in pore geometry will average out. It is assumed that an average behavior as indicated by the dashed line on Figure 40 will provide a reliable means for converting values of formation factor determined from electrical surveys to porosity. This dashed line is described by the equation:

$$F = 3.5\,\phi^{-1.8}$$

The samples used in compiling Figure 40 may not be representative of rocks at depth beneath Kilauea Volcano. It is possible that alteration of older volcanic rocks can modify the pore structures so that such rocks may more closely resemble sandstones in their electrical behavior. Samples of rock from depths as great as 4000 feet have now been obtained in the Kilauea Geothermal Test Hole, but the necessary resistivity determinations have not yet been completed.

This relationship between rock resistivity and water content is of value in geothermal prospecting only insofar as the water resistivity can be determined and the temperature inferred from this information. The resistivity of an aqueous electrolyte depends on the amount of salt in solution, the types of salt ions present, and the temperature. Inasmuch as the resistivity surveys show the porous section of volcanics to extend approximately two kilometers beneath sea level in the areas where they have low resistivities, it is quite probable that these rocks are saturated with sea water containing primarily sodium chloride in solution. Sea water normally has a resistivity of 0.25 to 0.30 ohm-meters at a temperature of 20° C. At higher temperatures, the resistivity decreases as shown by the curves in Figure 41, providing that there is sufficient pressure that the water does not change to steam. At temperatures above 180° C., the resistivity of sea water is 0.025 to 0.040 ohm-meters.

In order to estimate the rock resistivity which would correspond to this water resistivity, it is necessary to know the average porosity at a depth of 1 to 2 kilometers. As may be seen from the data contained on Figure 40, porosity determinations made on small samples show a very wide range, from

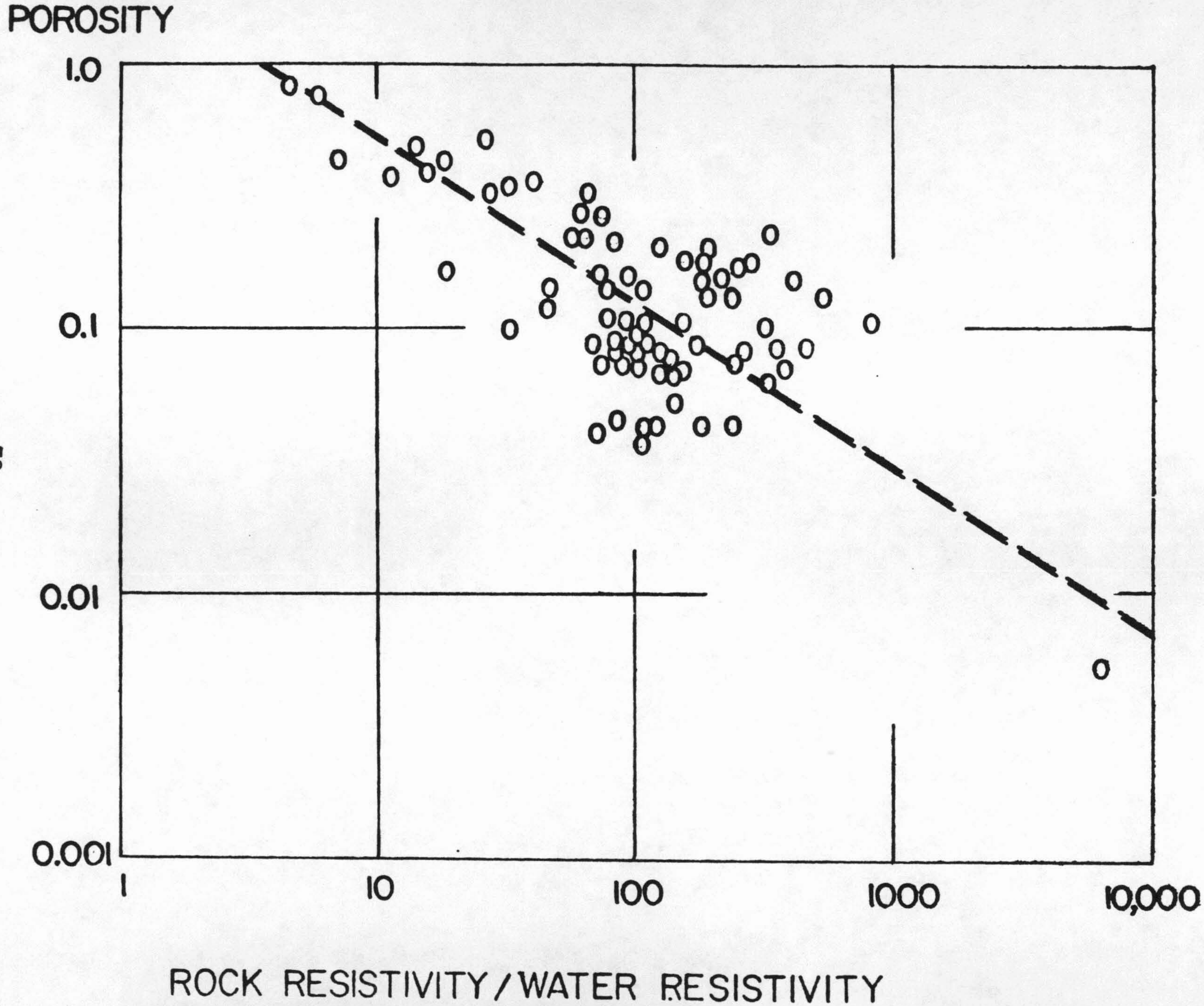

Figure 40. Relation between formation factor and amount of water-filled porosity for basalt samples from Hawaii.

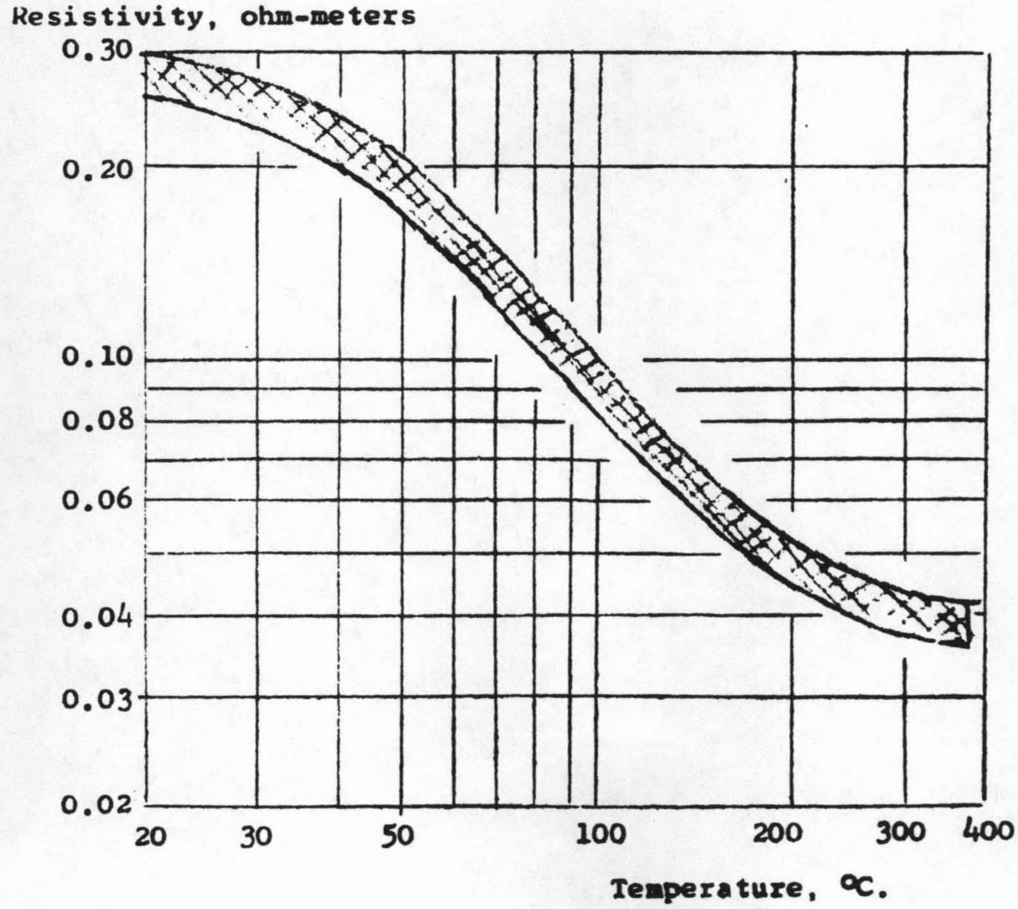

Figure 41. Relationship between the electrical resistivity of sea water and temperature.

less than 10 percent to over 50 percent. However, the high values of porosity seen with surface samples may not be present at depth because overburden pressures will tend to close the highly porous flows. A better estimate of average porosity is available from neutron irradiation well logs made in the Kilauea Geothermal Test Hole. These show the porosity at a depth of a kilometer or so to be reasonably uniform, and lie between 20 and 25 percent. Using the formation factor relationship shown on Figure 40, the formation factors corresponding to porosities of 20 and 25 percent are 42 and 30, respectively. In order to have temperatures in excess of 180°, we must have rock resistivities below 1.7 ohm meters for a porosity of 20 percent, and below 1.2 ohm-meters for a porosity of 25 percent.

The lowest resistivities actually observed were approximately 2 ohm-meters, in several anomalous areas along the lower part of the East Rift of Kilauea. Considering that the resistivity measured with a dipole survey is likely to be somewhat higher than the actual resistivity in a conductive anomaly, this result is highly suggestive that temperatures at depth in the anomalous areas may be as high as 180° C.

The validity of this conclusion is dependent on the reliability of our estimate of the probable porosity at depth. Some check is available in the form of resistivity data from the areas adjacent to the anomalous areas. In these regions, resistivities of 7 to 8 ohm-meters appear to extend to a depth of about 2 kilometers below sea level. Again assuming that the porosity at depth is 20 to 25 percent, the formation factors will be unchanged, being 42 and 30 respectively. The corresponding water resistivity is 0.16 to 0.25 ohm-meters. These water resistivities correspond to temperatures in the range from 30° to 60° C. This is a very reasonable temperature range for a depth up to two kilometers in an area with a thermal gradient of 20° per kilometer and an average surface temperature of 20° C. Thus, both the absolute value of resistivity observed in the areas of anomalously low resistivity, and the contrast between the low values of resistivity and more normal values of resistivity in adjacent areas are compatible with the existence of geothermal reservoir to depths of about two kilometers, with temperatures of 180° or more.

No resistivity determinations below approximately 10 ohmmeters were obtained over the summit area of Kilauea Volcano, where it is believed a geothermal system is present at depths of one to two kilometers below the surface. The reason appears to be that the pore waters involved in the geothermal system beneath the summit involves primarily fresh waters, with only enough salinity to correspond to 10 to 20 percent sea water mixed in. The lower content of sea water in the rocks penetrated by the Kilauea Geothermal Test Hole is probably a result of the great distance from the ocean, and the relatively large supply of surface waters in the area from the flanks of Mauna Loa. The dipole resistivity data indicate that resistivities at depth under the flanks of Mauna Loa and in the Mountain View-Glenwood area are 20 to 50 ohm-meters. The contrast between these values and the 10 ohm-meters seen under the summit of Kilauea is fully compatible with a temperature at depth of 30 to 50° C in the areas outside the summit anomaly, and the 150° or higher temperature known to exist below sea-level at the Kilauea Geothermal Test Hole.

In summary, there is a good possibility that commercial geothermal fluids can exist at depths up to two kilometers in several areas of anomalously low electrical resistivity along the lower part of the East Rift of Kilauea. However, it must be stressed that various combinations of factors other than temperature may be causing the low resistivities to be present, such as local increases in the porosity of rocks at depth, or local salinity concentrations greater than that of sea water. It is recommended that further detailed geophysical and geological studies be carried out in the vicinity of the anomalies mapped during this survey to further confirm the nature of the anomalies, and to provide more definitive information for siting test holes in the best locations. Among the additional studies that might prove worthwhile are:

1. Detailed electrical soundings using both the Schlumberger direct-current sounding method and the electromagnetic sounding method to better define both the vertical and horizontal limits of the areas with low resistivity.

2. Detailed gravity surveys to assist in determining the density of rocks within the areas of low resistivity, and thus provide a check on the temperature estimates made here.

3. Detailed microseismicity studies to help locate fault planes and shear zones where fluid permeabilities will be higher than normal, to provide an optimum capacity for producing fluids if the resistivity anomalies do indeed correspond to geothermal reservoirs.

4. Surveys of ambient seismic noise, to determine if sufficient underground movement of water is taking place in the low resistivity zones to be detectable.

Other surveys that may also be helpful in siting testholes would involve detailed studies of fractures in the vicinity of the resistivity anomalies and an inventory of the discharge of warm waters in wells and along the sea coast.